ISSN 2631-4843

The British Astronomical Association

Variable Star Section Circular

No. 196 June 2023

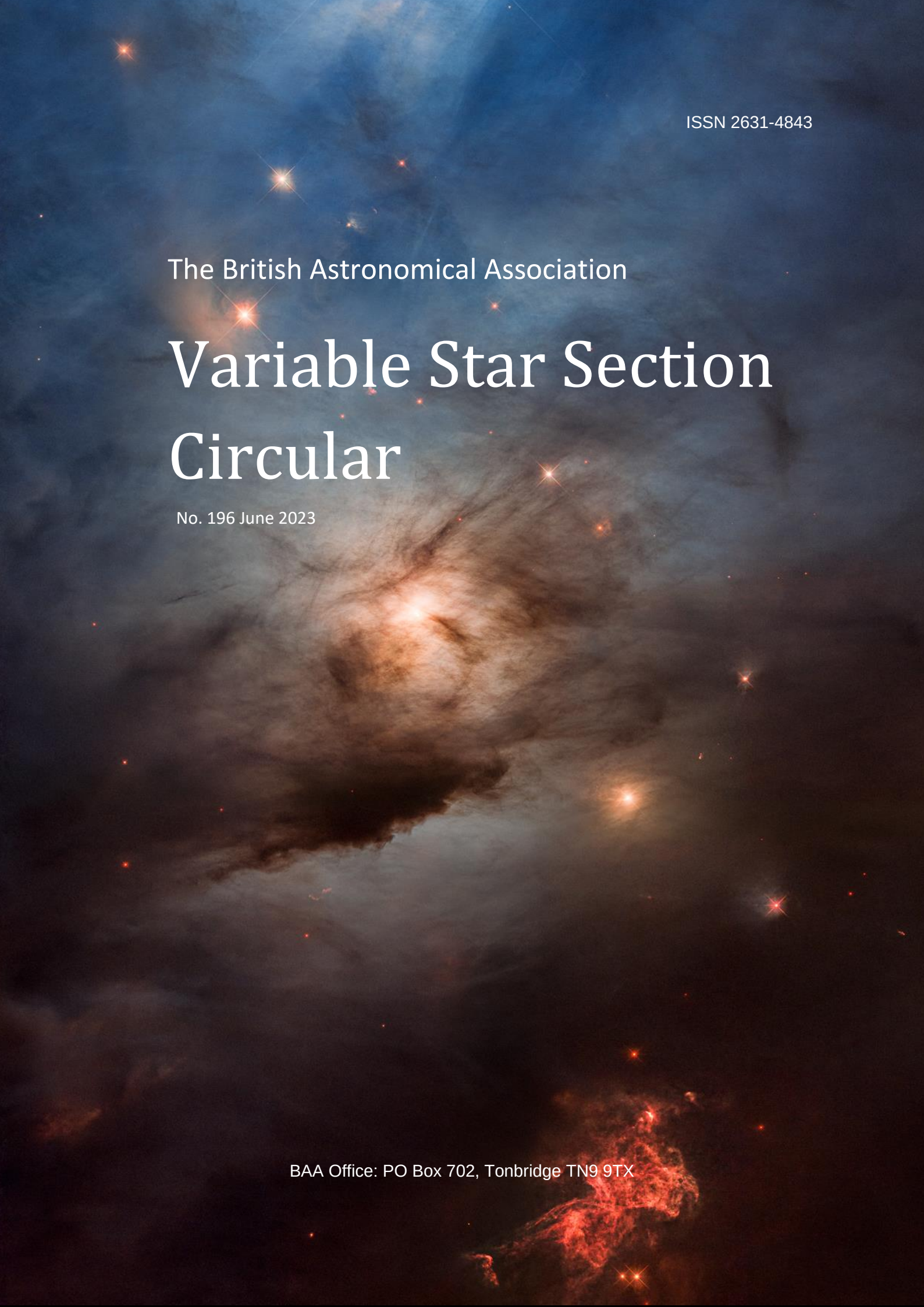

BAA Office: PO Box 702, Tonbridge TN9 9TX

Contents

Cover Picture

Part of the Perseus molecular cloud and OB-2 association,
HD 281159 and the reflection nebula vdB 19 and NGC 1333

NASA/ESA/STScI
See page 39.

From the Director — *Jeremy Shears*

Section meeting on 2023 September 2

I hope to see many of you at our Section meeting on Saturday September 2. It will be held at the Humfrey Rooms in Northampton, courtesy of the Northamptonshire Natural History Society. We have a full line up of speakers on all aspects of variable star astronomy: further information elsewhere in this Circular. A light buffet lunch will be provided, as well as tea and coffee during the day. Entrance, including these refreshments, is free of charge and no advanced booking is necessary.

One of the main points of the Section meeting is to gather in person to discuss projects and ideas together - especially after such a long period of being unable to meet. Hence, we have no plans to live-stream or record the meeting.

2023 BAA Winchester Weekend

Another very enjoyable Winchester Weekend was held in mid-April at Sparsholt College. There were quite a few VS observers present and on the Saturday morning we enjoyed an excellent talk by Gary Poyner about the long-standing pro-am collaborations on the enigmatic binary black hole, OJ 287.

The new VSS display boards were used to highlight observers' projects. Many thanks to Kevin Gurney, David Boyd, Colin Henshaw and Gary Poyner for providing display material.

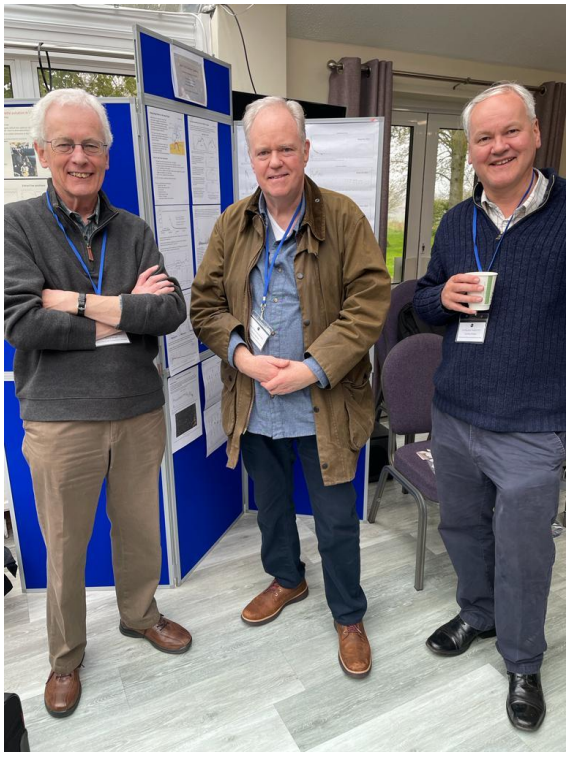

David Boyd, Kevin Gurney and the Director at the VSS display at Winchester.

(photo by Gary Poyner)

A short period of clear sky on the Saturday evening allowed telescopes to be set up and some observations to be made. In a nod to VS observing, Chris Lloyd and the Director estimated the magnitude of Betelgeuse before retiring to the bar.

VLF detection of Gamma Ray Burst GRB 221009A

BAA Radio Astronomy Section member, John Cook, reports that on 2022 October 9 the Fermi and Swift Gamma ray satellites both detected an extremely strong GRB at 13:16:59 UT, while the STIX X-ray satellite recorded an X-ray signal just three minutes later. The sun was not flaring at this time, but John's VLF detector recorded a Sudden Ionospheric Disturbance (SID) which he attributes to the GRB. The plot below shows his recording of the GRB and compares it with a normal (ordinary) solar flare.

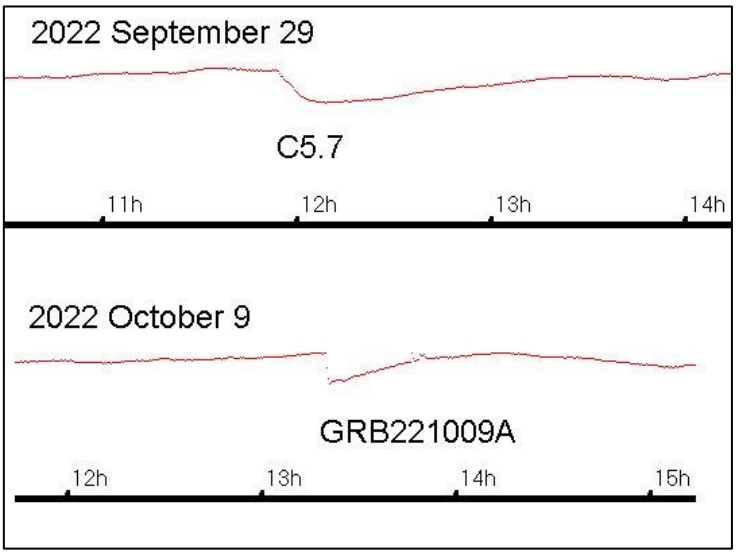

John Cook's VLF recording of GRB 221009A compared to an ordinary C5.7 solar flare.

The GRB SID was also detected by Paul Hyde, Mark Edwards and Roberto Battaiola. Professional analysis located the source of the GRB to be in the constellation of Sagitta. Further details can be found in the Radio Astronomy Section's "Radio Sky News" for 2022 October.

T CrB

Anticipation is rising about the next eruption of the recurrent nova. There have been a few ATels recently discussing its current super-active state. John Toone has an article about it in this Circular. I will be giving a talk "Get set for the next eruption of the recurrent nova, T Coronae Borealis!" at the next BAA meeting, which will be held in London on June 7, https://britastro.org/event/alcock-2023. I hope to see some of you there.

Patrick Schmeer (1964 – 2022)

No doubt like many others in the variable star community, I was shocked and saddened to learn that Patrick Schmeer had passed away on 9 August 2022. He was a dedicated and enthusiastic visual observer of variable stars from his home in Bischmisheim, Germany. He was especially interested in members of the cataclysmic family. Observationally, he specialised in patrolling for outbursts of dwarf novae and other eruptive stars. Patrick was renowned for his prompt detection of many rare outbursts as well as confirmation of other transient objects posted on the CBAT transients webpage. Along with

Gary Poyner, for many years he managed the CVnet Cataclysmic Variables Network webpages. He was also an active member of the team managing the AAVSO's International Variable Star Index (VSX).

On behalf of the BAA VSS, I send our condolences to Patrick's family and friends.

Patrick Schmeer (image from his AAVSO online profile)

Brian Warner (1939-2023)

I was also very sorry to learn of the death of Professor Brian Warner at the age of 83. He was one of the most distinguished astronomers in South Africa, and his name is synonymous with astronomy at the University of Cape Town, where he was the founding Chair of Astronomy on his arrival in 1972. He held the post for 33 years until his retirement in 2004. Brian was a pioneer of high-speed photometry of cataclysmic variable stars. His book published by Cambridge University Press, "Cataclysmic Variable Stars", remains a classic and one to which I refer quite often. I am sure many CV enthusiasts have it on their shelves. I had the pleasure of meeting Brian twice and each time he was very encouraging about amateur contributions to CV astronomy.

Professor Brian Warner after receiving the award of DSc (honoris causa) from the University of Cape Town in 2009. Credit: University of Cape Town

CV & E News

Gary Poyner

garypoyner@gmail.com

Recent activity in programme stars SU Tau, AO Her, V1251 Cyg and MV Lyr are covered.

SU Tau:

Following vsnet-alert 27582 issued by Taichi Kato on April 2nd and posted to BAAVSS-alert the same day regarding the fading of the RCB star SU Tau, observations reported to the BAAVSS database up to April 28 (the last data point in the database at time of writing) show the fade to have been a short duration event, reaching a minimum of only 14.7CV on April 19, before returning to magnitude 11.5CV nine days later on April 28.9 UT.

SU Tau has one of the largest amplitudes of all RCB stars, being in excess of 10 magnitudes in V.

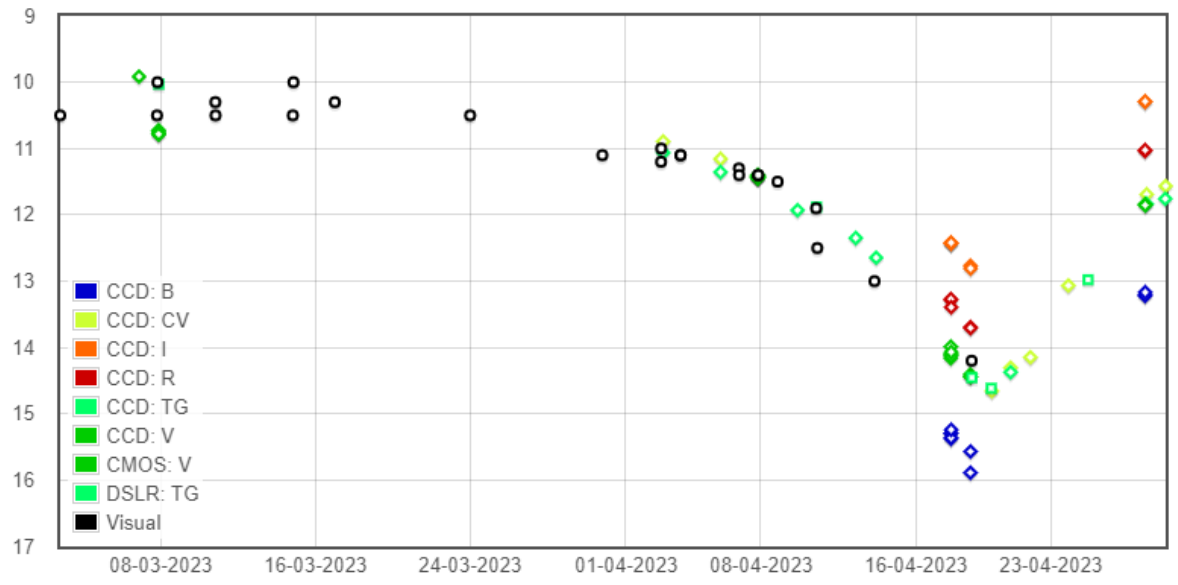

SU Tau. March 1st – April 28th, 2023. BAAVSS database. Observers LK Brundle, G Fleming, M Larsson, PC Leyland, W Parkes, G Poyner, J Toone & I Walton.

AO Her:

This rather neglected RCB star is currently in deep minimum, having begun its current fade in mid-March 2023 (when observations are sparse) from its maximum brightness of 10.5V mean. Currently at magnitude 17.3CV, it still has nearly two magnitudes to go to reach its deepest level of 19.0V recorded during the 2015 minimum. Previous recorded minima show that the star doesn't spend long periods at low state and begins to recover in just a few months. These recovery times (from min to max) are generally slow and can take a year to reach maximum brightness from a deep minimum.

If you like observing RCB stars (and who doesn't?), please add this object to your programme and monitor it on every possible occasion.

V1251 Cyg:

A rare outburst of the UGWZ star V1251 Cyg was detected by Masayuki Moriyama on March 28.794 at magnitude 14.29C. Taichi Kato comments on vsnet-alert 27563, that this was the first recorded outburst since 2008. However, the AAVSO light curve shows an outburst in September 2013 with two data points from different observers, peaking at visual magnitude 14.4 on Sep 08, and a single TG datapoint on June 30, 2014 at magnitude 14.87. The timings of both of these 'outbursts' are however, completely out of character for UGWZ type stars.

Using VSNET data from various 'activity at a glance' reports sent out by Kato, we can say that the March '23 outburst lasted 21d and peaked at magnitude 12.77V on March 29.78.

MV Lyr:

In VSSC 193 & 194 I wrote about the current activity in the NL star MY Lyr, and its most recent low state reached in October and November 2022. At some stage during the seasonal gap of November – February, the recovery began with MV Lyr being picked up on 2023 Feb 19 at magnitude 15.0CV (over 2 mags brighter than in November) and rising slowly. At the time of writing (May 18), MV has recovered to magnitude 13.0mv, and is now close to its maximum levels of 12.0-12.5V. These fading events are like RCB fades – unpredictable, so please keep MV Lyr under close watch this observing season. Charts are available from the AAVSO

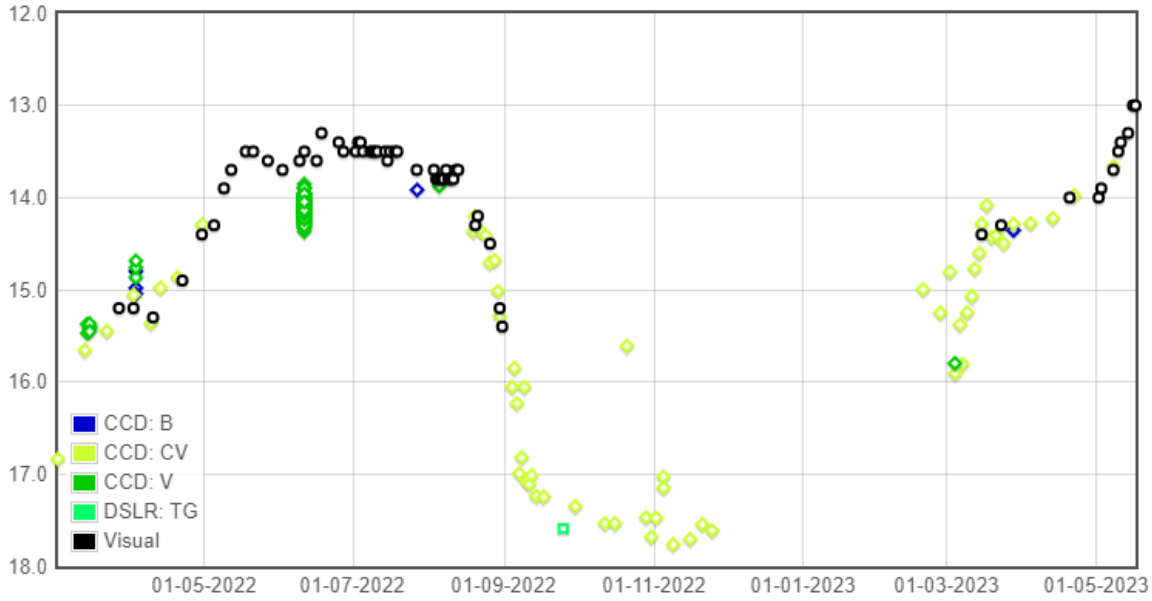

MV Lyr Jan 01, 2022 – May 18 2023. Observers P Bouchier, S Johnston, W Parkes, G Poyner & I Walton.

V1413 Aql:

As you read these words, the 2023 eclipse of this symbiotic star should be well under way, with AAVSO VSX predicting a mid-eclipse date of June 11, 2023. Hopefully the weather will be kind enough for observations to be made and a report to appear here in the next VSSC in September.

T Coronae Borealis – The Pre-Eruption Dip

John Toone

enootnhoj@btinternet.com

A change in form of variation is reported for T CrB that may indicate that a pre-eruption dip has commenced. Also, the BAA VSS chart for T CrB has been revised to cover a potential fade to magnitude 12.

T CrB entered a high active state in April 2015 [1] and there has been much speculation that this event is a precursor to the next outburst of the brightest of the recurrent novae which previously erupted in 1866 and 1946.

Based on an analysis of B & V (V converted from visual) data leading up to the 1946 eruption, Bradley Schaefer has made a prediction for the next outburst. [2] Schaefer proposes that if the star follows the same pattern as before there will be a pre-eruption dip directly following the ongoing high state which will commence roughly one year ahead of the eruption and the lowest part of the dip will be approximately three months in advance of the eruption.

Schaefer's historical light curve indicates that a previous high active state occurred from early 1937 to the end of 1944 and the dip followed in 1945 leading up to the eruption in early February 1946. An interesting aspect of the pre-eruption dip was that it was much greater in range in V than B and possibly dropping to magnitude 12, a full magnitude below quiescence level.

The outline visual variation of T CrB since 1981 is given in Figure 1. Throughout this 42-year period the range was roughly within a band of 1 magnitude of which ellipsoidal variation accounts for more than half. The light curve also indicates that elevated activity occurred in 1982-1986 & 1996-1999 in addition to the high state activity apparent since 2015. Just prior to the high active state in 2010-2014 the variation ranged between 10.3-10.9mv with relatively smooth ellipsoidal variation which is a common feature of the T CrB system.

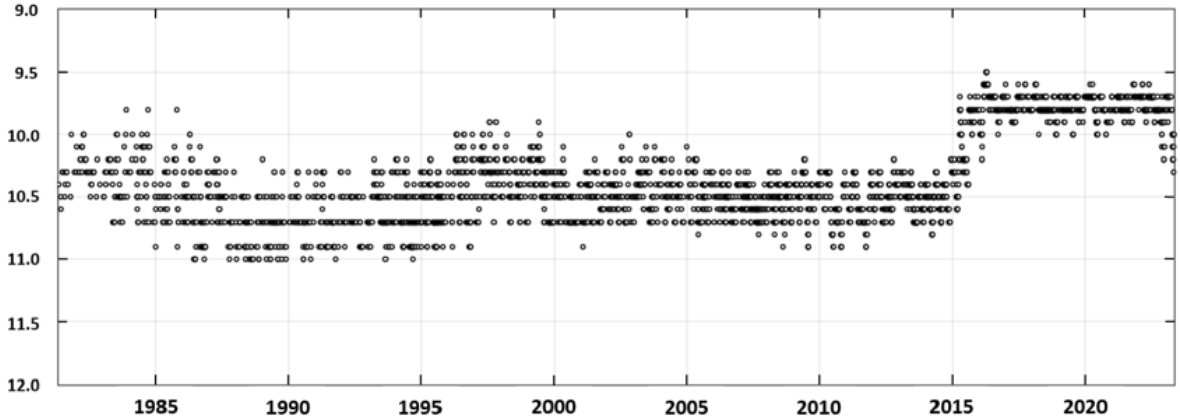

Figure 1: Light curve of T CrB drawn from 3928 nights of visual observations undertaken by the author between May 1981 and April 2023. During quiescence the visual data shown here is systematically 0.4 magnitude fainter than equivalent V data due to the fact that the variable is redder than the comparison stars. However, during the high active state the colour of T CrB becomes rather blue and the systematic difference with V is eliminated.

After settling down in the high active state by mid-2016 the ellipsoidal variation resumed but it was less well defined compared with the quiescent state beforehand. The magnitude range throughout the high active state period from 2016 to 2022 was 9.6-10.0mv.

In November 2022 the behaviour started to change with the range shifting to 9.7-10.2mv and 0.2 magnitude flickering seen on the 14th November. [3] Then in April 2023 the variation further changed with the range dropping to 9.8-10.3mv and briefly dipping to 10.5mv during a flickering spell seen on the 23rd April. [4] This change in form of variation is visible on the extreme right of the light curve in Figure 1. In addition to the spells of flickering detected visually there has been smaller scale flickering reported in 2023 by S.N. Shore [5] and R.K. Zamanov. [6]

Enhanced flickering (within visual detection range) in conjunction with the increased variation range and reduction in mean magnitude, indicates that T CrB may be coming out of the high active state after eight years (the same duration as in 1937-1944) and has started the anticipated pre-eruption dip. Therefore, within the next 12 months we could be fortunate to witness a dramatic range of variation in the order of 10 magnitudes.

References:

1. 2016 BAA VSS Circular 169, 6-9.
2. 2023 MNRAS.tmp.729S
3. BAA VSS Alert, 14/11/2022 20:08GMT
4. BAA VSS Alert, 23/04/2023 22:13GMT
5. 2023 The Astronomer's Telegram 15916.
6. 2023 The Astronomer's Telegram 16023.

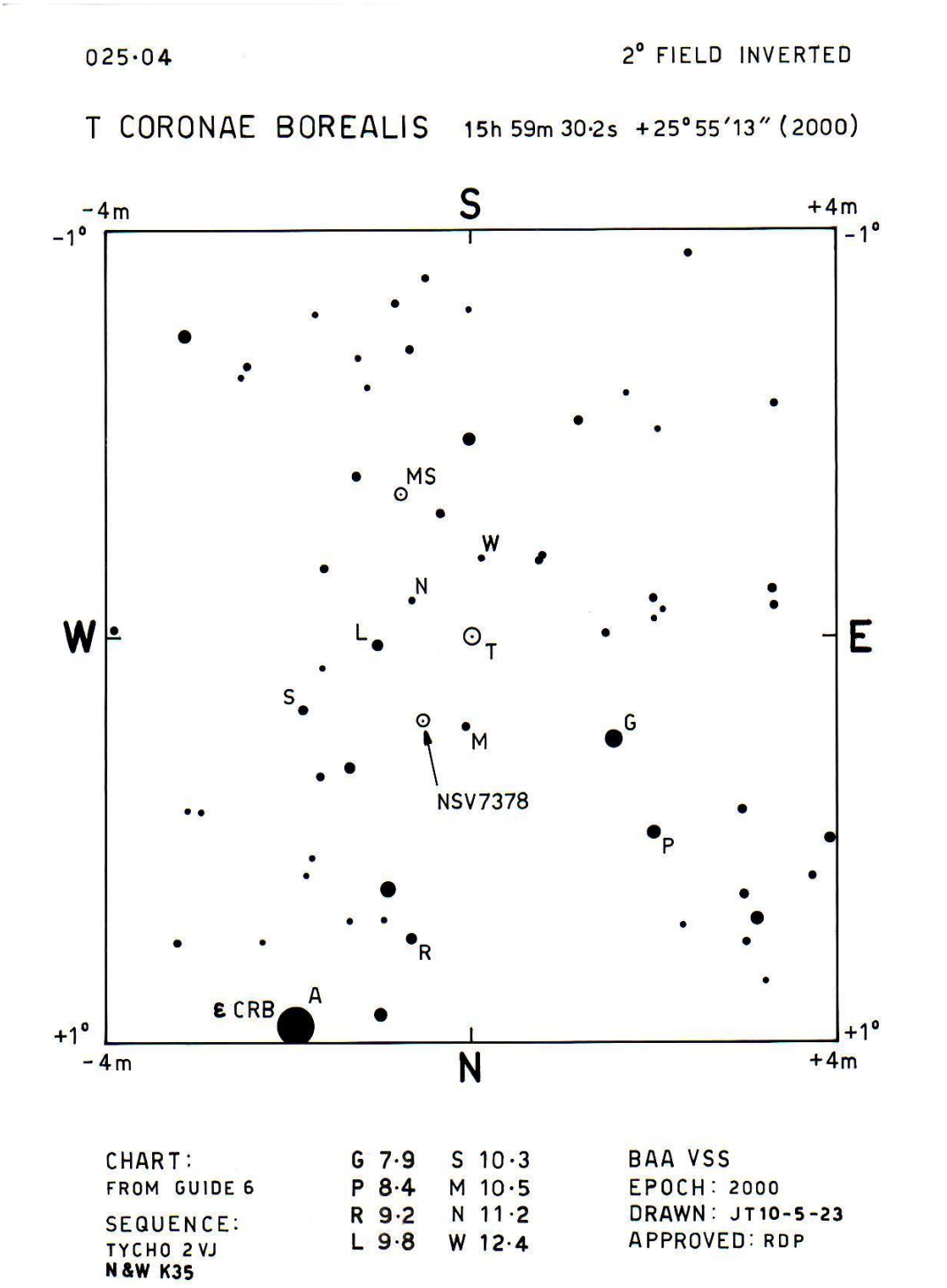

Figure 2: BAA VSS chart for T CrB for use by visual observers when the star is at minimum light. This chart has been revised to include comparison star W in case T CrB drops to magnitude 12 during a pre-eruption dip. When T CrB goes into full outburst additional wider field charts are available from the VSS Web-page. (*Click here to retrieve full size 2 degree chart from VSS web page*.)

Ian Miller's variable stars

Christopher Lloyd
cl57@ymail.com

Three new variable stars were discovered in the fields of CVs. V505 Scuti is a faint Mira variable with a P = 334 ± 1 d. GSC 02873-03309 is a low-amplitude W UMa eclipsing binary with a period of 0.4996319(2) d. The eclipses have depths of 0^{m}. 107 and 0^{m}. 102 in the TESS data suggesting a low inclination. GSC 03465-00810 is a short-period system with P = 0.27668359(4) d, but has a third body in a 4000 d orbit with a probable mass of 0.5 M showing a light-travel-time effect of 0.01 d.

Ian Miller (1946–2020 Furzehill Observatory website) was a long-term and prolific observer for the BAA VSS and the AAVSO who marked the journey of our time from visual observing with binoculars and larger telescopes to high-precision CCD photometry, and made a significant contribution in the process. His main focus was on cataclysmic variables and while observing some of these he discovered three new variables – that we know about – lurking in these fields. The first is now known as V505 Scuti, a faint Mira variable with $V \sim 14.5 - 15.0$ at maximum, and the other two are slightly brighter but essentially anonymous W Ursae Majoris systems, GSC 02873-03309 and GSC 03465-00810.

V505 Sct (USNO-B1.0 0857-0425370) was discovered in the field of the recurrent nova EU Scuti (Nova Sct 1949) while making observations as part of the VSS Recurrent Objects Programme. The initial observations were made unfiltered but calibrated as *V* (*CV*), and following discovery additional

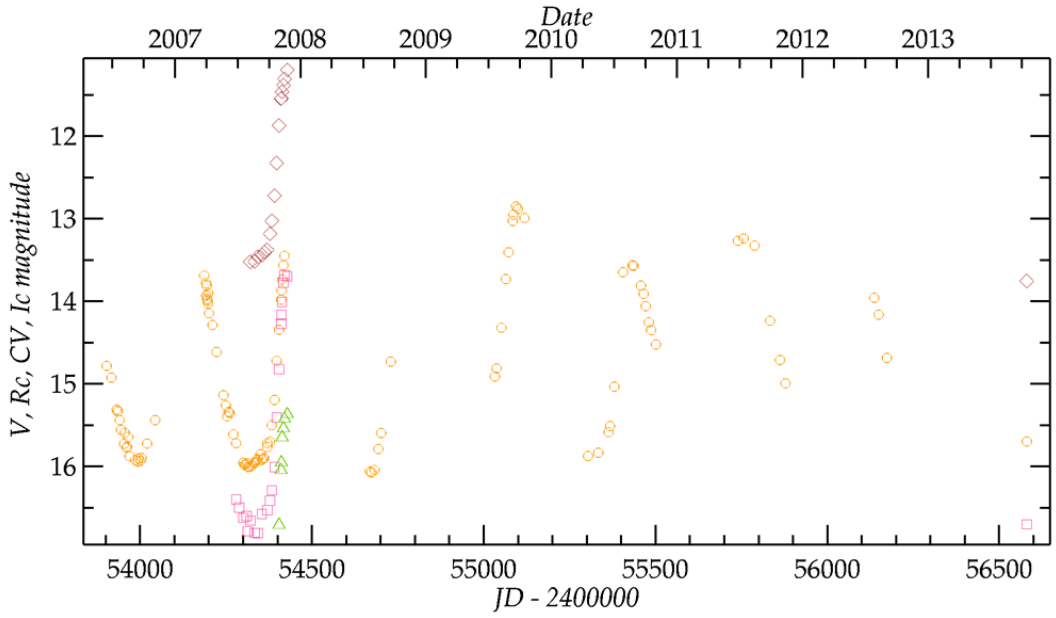

Figure 1: Epoch plot of Miller's observations of V505 Sct showing the *CV* data (circles), R_c data (squares) I_c data (diamonds), and a small number of *V* measurements (triangles). They show the enormous range in brightness with wavelength, and in particular the slightly redder-than-R_c effective wavelength of the *CV* magnitudes.

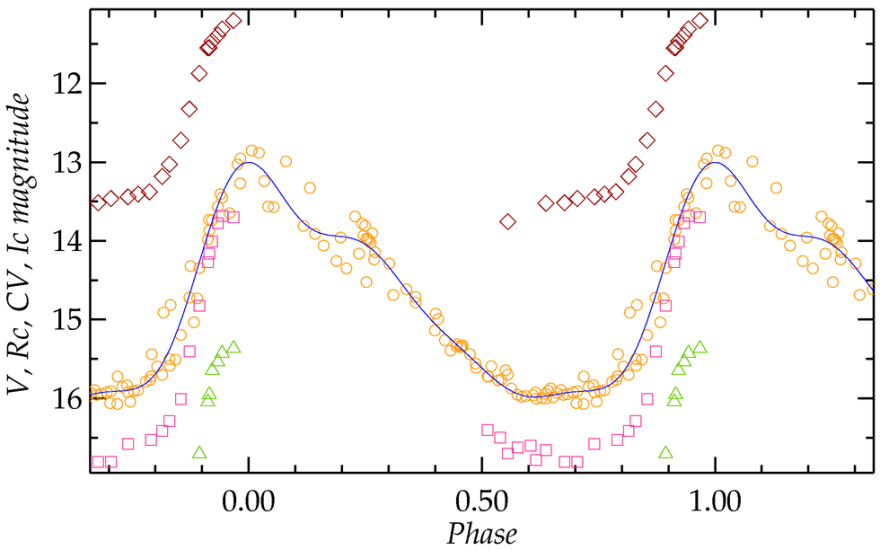

Figure 2: The phase diagram of Miller's observations of V505 Sct data folded on the best period for these data of 327 d. The mean 4-harmonic Fourier fit is shown for illustration and the symbols are as in Figure 1.

filtered observations were made in R_c and I_c, with a small number in V. These observations used the appropriate magnitudes for the bands but didn't include any second-order terms in the calibration. The majority of the observations were made in 2007 and Miller reported the results in the *Circular* at the end of that year [1] but limited and increasingly sparse observations continued over the following six years. Miller's full light-curve of V505 Sct is shown in Figure 1. Based on the first two seasons Miller suggested a period of 335 d but a 4-harmonic Fourier fit to all the data finds the best fit with a period of 327 d, and a plot of the data folded on this period is shown in Figure 2. The full amplitude of the variation is $\sim 2^m.5$ in I_c, $\sim 2^m.9$ in CV and $\sim 3^m.3$ in R_c, so it is clearly a Mira variable.

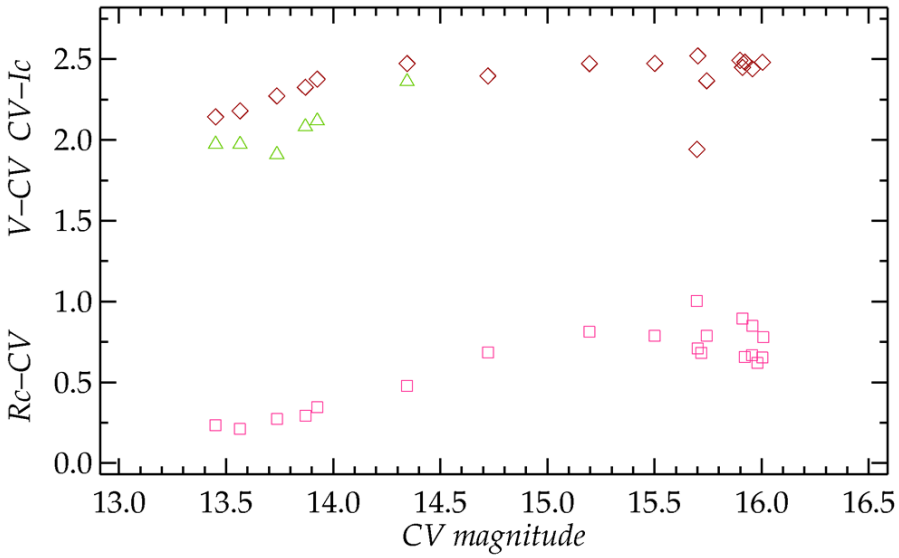

Figure 3: The magnitude differences of Miller's contemporaneous filtered observations in the sense (bluer–redder) for ($V - CV$), ($R_c - CV$), and ($CV - I_c$) as a function of CV. The absolute level simply depends on the magnitude chosen for the CV calibration. The trend towards redder colours at fainter magnitudes confirms that CV is effectively redder than R_c, and this is supported by the lower amplitude in CV as well.

Miller noted the difference between *V* and *CV* magnitudes and this highlights the impact of the very red colour of the variable on the effective wavelength of the unfiltered observations. In fact, these would be more appropriately calibrated using the R_c magnitudes of the comparison stars, but the effective wavelength of the unfiltered observations actually lies to the red of R_c. A plot of the magnitude differences of the contemporaneous filtered observations in the sense (bluer–redder) is shown for ($V - CV$), ($R_c - CV$), and ($CV - I_c$) as a function of *CV* in Figure 3. All the colours become redder as the star fades so they are calculated in the correct sense. Also, the amplitude of the star decreases towards the red and this places the effective wavelength of *CV* between R_c and I_c.

The star has since been reported as variable in data from the All-Sky Automated Survey for Supernovae (ASAS-SN) project [2, 3], the Asteroid Terrestrial-Impact Last Alert System (ATLAS) project [4, 5] and the Zwicky Transient Facility (ZTF) [6, 7]. As the star is relatively faint the ASAS-SN data cover only the maxima, which are ∼14.5–15.0 in *V* and ∼15.5 in the Sloan *g*-band. The limited data suggest a period of 335 d for the data since 2015. More extensive data are available from the ATLAS project covering the full amplitude range of the variable. ATLAS data are given in two overlapping, largely rectangular photometric bands. The 'cyan' band covers the wavelength 4200–6500 Å, broadly similar to the combined Sloan *g* and Johnson *V* bands, while the 'orange' band covers the range 5600–8200 Å, corresponding well to the Sloan *r* and *i* bands, with the overlap in the *r* and R_c bands. The most complete coverage is available in the 'orange' data from late 2015 while the 'cyan' band provides much sparser coverage but increasing with time. The ATLAS light-curve since 2015 is shown in Figure 4 and the individual cycles are obvious, as is the difference in amplitude between the two bands, which reflects the change in temperature as well as radius. The phase diagram of the ATLAS data is shown in Figure 5 and it seems likely that the minima are at the limit of the data, as the observations are much less consistent. The ZTF data are only available from 2018 but are generally more sensitive so probably show the full amplitude in the ZTF *g* and *r* bands. The epoch plot and phase diagram are shown in Figure 6. The 4-harmonic Fourier fits to the individual ATLAS and ZTF filter data give very consistent ephemerides for the time of maximum light – but they do largely cover the same time interval – however the amplitudes and coverage are very different. The best ephemeris of maximum light is

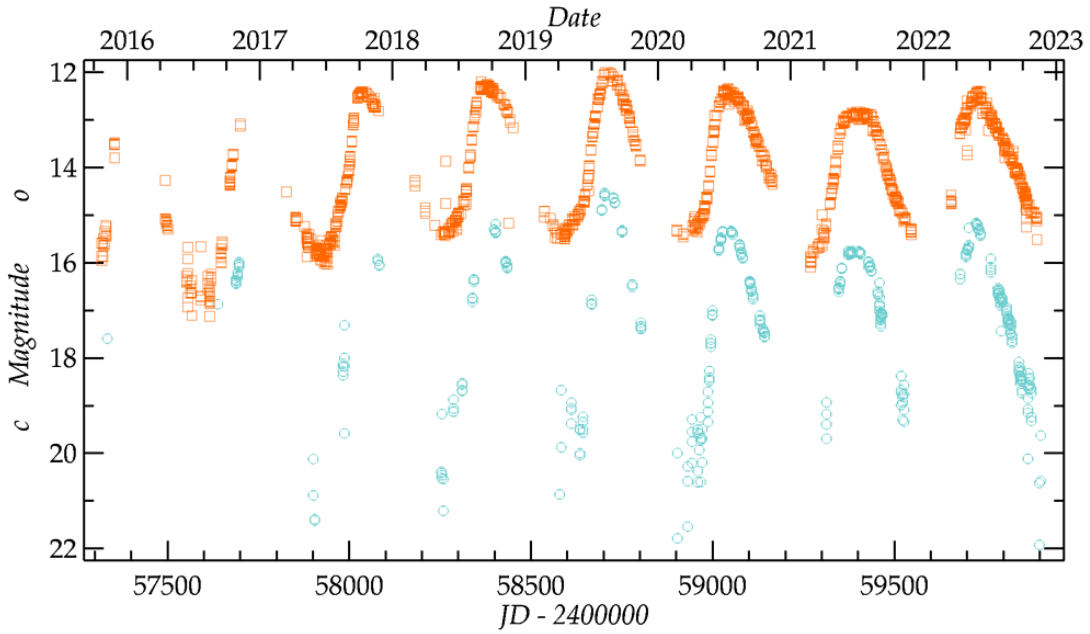

Figure 4: Epoch plot of the ATLAS orange- (upper) and cyan-band (lower) data again demonstrating the increase in amplitude towards the blue.

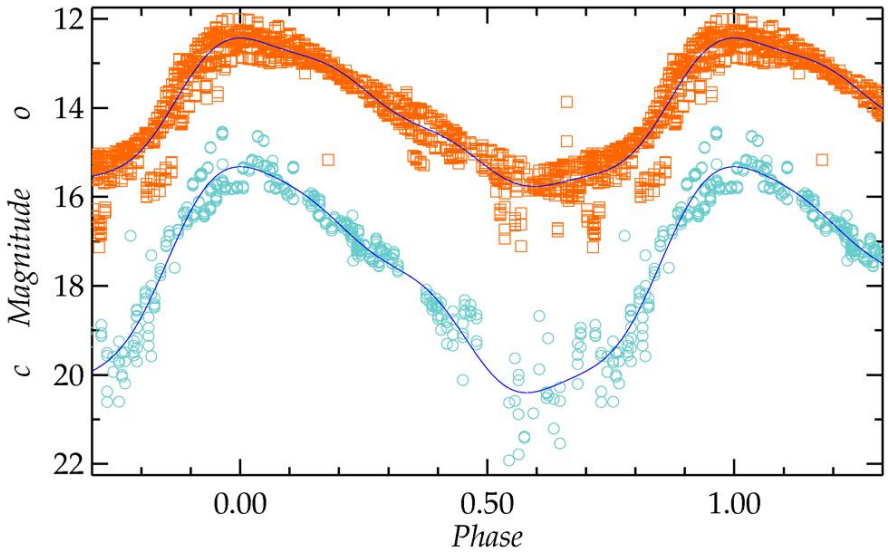

Figure 5: The phase diagram of the ATLAS orange- (upper) and cyan-band (lower) data folded on a period of 334 d.

$$JD_{Max} = 2458708 \pm 2 + 334 \pm 1 \times E \qquad (1)$$

where the uncertainties are suggestive. Obviously, there is much larger variation in the timing of individual maxima but the ephemeris should be reliable at this level. Over time there may also be

larger changes as the best period between the recent and Miller's data suggests a period of 328 d, but this is based on much less data at the earlier epoch.

The second of Miller's discoveries is GSC 02873-03309 (UCAC4 671-018057) which he identified as a low-amplitude W Ursae Majoris variable [8] while making time-series observations of the UGSU variable SDSS J032015.29+441059.3. The star has $V \sim 13.9$ with an amplitude of $0^m.1$, and a period very close to half a day. The initial observations were made during October 2016 and a further run was made in January 2018 to complete the phase diagram. The star has also been observed by

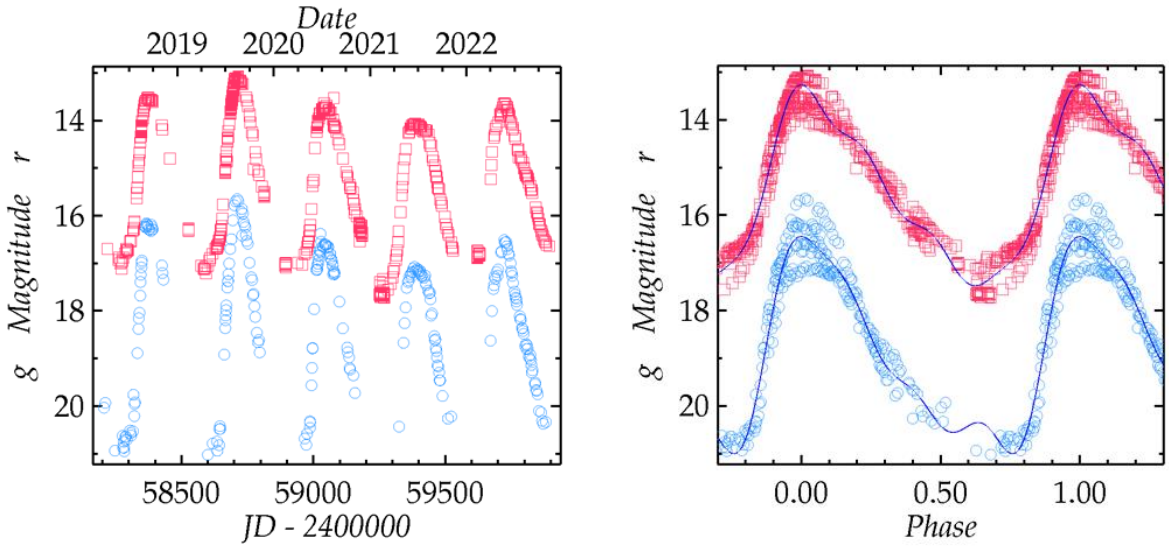

Figure 6: (left) Epoch plot of the ZTF *g* and *r* data of V505 Sct, and (right) the corresponding phase diagram folded on a period of 334 d.

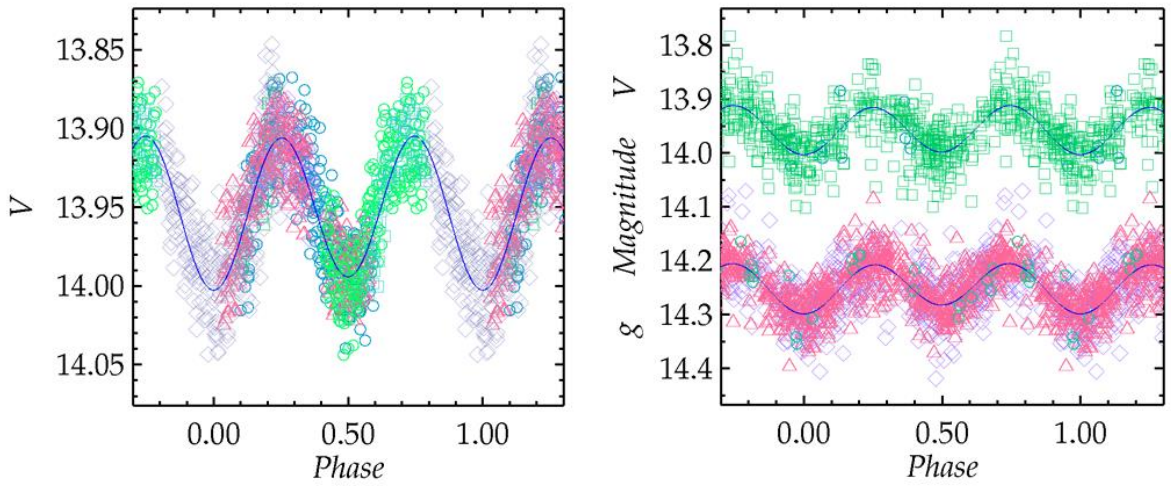

Figure 7: The phase diagrams of (left) Miller's time-series *V* data and (right) the ASAS-SN *V* - and *g*-band data folded of the ephemeris in Equation 2. The different symbols indicate different runs in Miller's *V* data and different cameras in the ASAS-SN *g* data.

ASAS-SN, ATLAS and ZTF but because it is relatively faint, $V \sim 13.9$, and the amplitude is low, and the period is very inconvenient, the phase diagrams of subsets of the data do not provide coverage of some of the minima, so it is difficult to make eclipse timings. The phase diagrams of the complete data sets are shown in Figures 7 and 8 where some of the problems with noise and sparse phase coverage can be seen. GSC 02873-03309 has also been observed by the Transiting Exoplanet Survey Satellite (TESS) [9] during November 2019 in Sector 18 at the standard 30-minute cadence, and during November 2022 in Sector 58 with a much higher cadence of 200 seconds. However, the light-curve is compromised by high background noise and a nearby star, so the scatter is larger than would normally be expected, and for TESS the star is on the faint side. The phase diagram is shown in Figure 9 with a 4-harmonic Fourier fit. There is no systematic deviation from the mean light-curve and the residuals have a rms error of $0^m.012$. The amplitudes of primary and secondary eclipses are $0^m.107$ and $0^m.102$, and the maxima are the same to $0^m.001$. All the timing data suggest that the period is constant with an ephemeris of primary minimum of

$$HJD_{\mathrm{MinI}} = 2458796.50647(30) + 0.49963190(18) \times E \qquad (2)$$

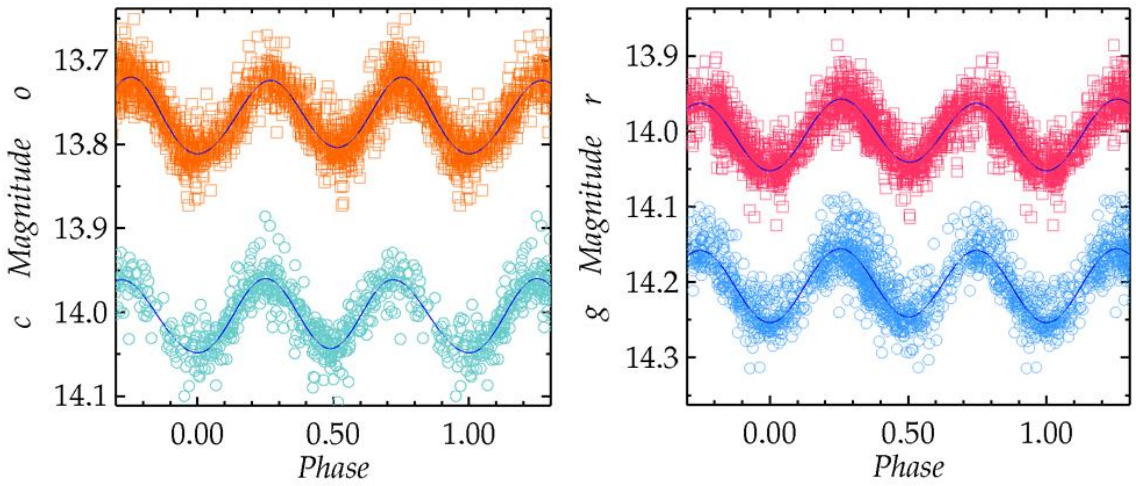

Figure 8: The phase diagrams of (left) The ATLAS 'orange' (*o*) and 'cyan' (*c*) data, and (right) the ZTF *g* and *r* data, with the *r* data offset by $-0^m.2$ from the *g* data. All the other bands are shown at the correct level.

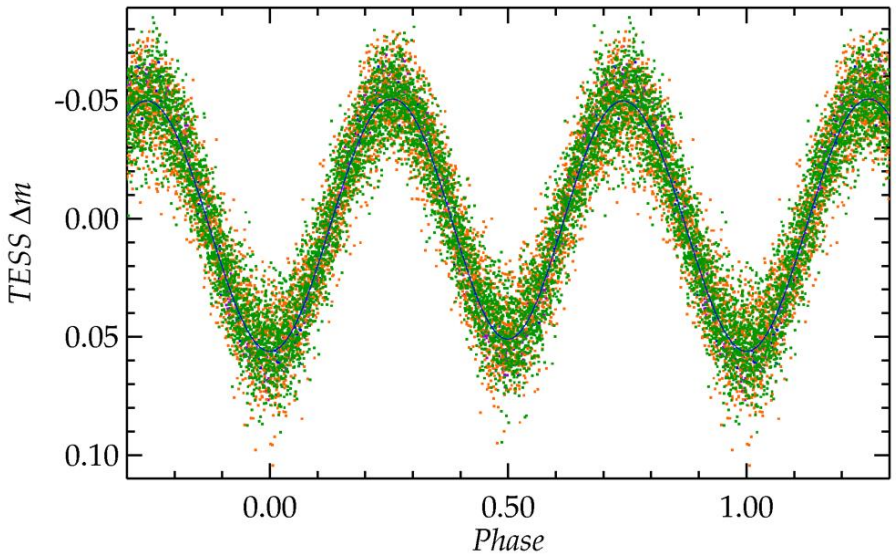

Figure 9: The phase diagram of the TESS data folded on the best fit period given in Equation 2. The different half-sectors are shown in different colours.

so, there is no obvious sign of a third companion, which are fairly frequent in W UMa systems.

The period of GSC 02873-03309 lies at the break point of the empirical Period-Luminosity relationship between the early- and late-type W UMa systems (see e.g., Jayasinghe et al. [10]), and broadly corresponds to the transition region between the more rapidly and slowly rotating main-sequence stars, referred to as the Kraft break [11], which occurs over the temperature range $T_{\rm eff} \sim 6200–6700$ K. Period-Luminosity relationships for both the early- and late-type populations suggest that the absolute magnitude of the system is $M_V \approx 2.4$ and $M_G \approx 2.4$, and these are broadly consistent the absolute magnitudes derived from the observed V and G magnitudes, the reddening, and the

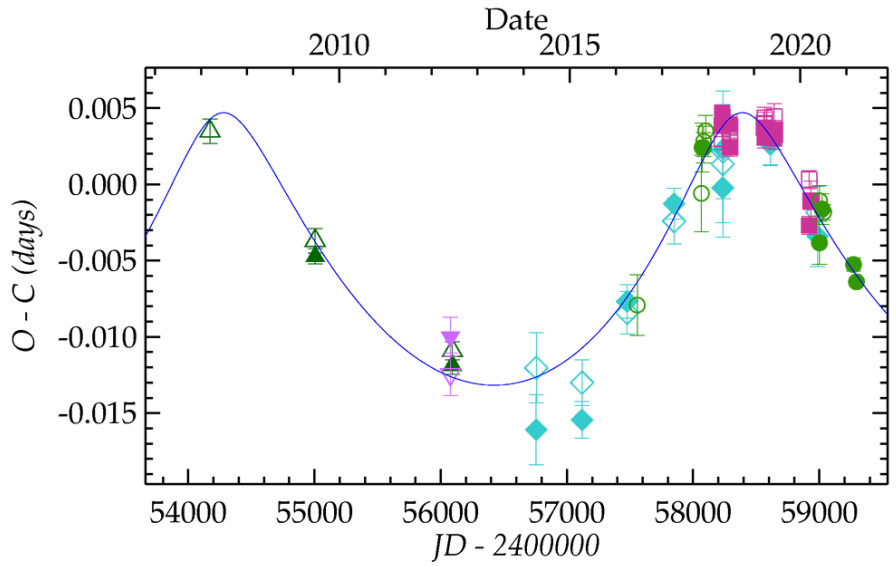

Figure 10: The O-C diagram of GSC 03465-00810 showing the weighted LTTE fit. The symbols identify the different data sets; CSS (upward triangles), Pan-STARRS (downward triangles), ASAS-SN (diamonds), ZTF (squares), and time-series data (circles). Open symbols identify secondary minima.

distance. So, the shallow eclipses are most likely caused by low inclination, and not through dilution by the presence of a luminous third body. The *Gaia* DR3 Apsis processing based on the reddening and the BP/RP spectra gives T_{eff} = 6492 K and different LAMOST spectral calibrations also give T_{eff} ~ 6600 K [12]. The empirical effective temperature calibrations for the two populations suggest that at P = 0.5 d, T_{eff} = 7041 or 6596 K respectively so despite its relatively long period it is more consistent with the cool-star calibration. A detailed description of this system has been published recently [13].

The last of Miller's discoveries is GSC 03465-00810 which he originally identified as a W UMa variable while making observations of the UGWZ candidate ASASSN-16fy [14]. The initial timeseries observations were made over ten nights between June 2016 and December 2017 and from these there was already a suspicion that the period was variable. Supplementary observations were made by Daryl Janzen at the University of Saskatchewan's Department of Physics and Engineering Physics Sleaford Observatory, and Yenal Öğmen of the Green Island Observatory, Northern Cyprus, during 2020 and 2021. The star has also been comprehensively observed by the ASAS-SN project, the ZTF project, and the Catalina Sky Survey (CSS), which pre-date Miller's observations.

GSC 03465-00810 has V ~ 14.8 so it is significantly fainter than the previous W UMa system, and the amplitude is also relatively low at $0^m.3$. Hoverer, the period is short at $0^d.277$ and so is a better

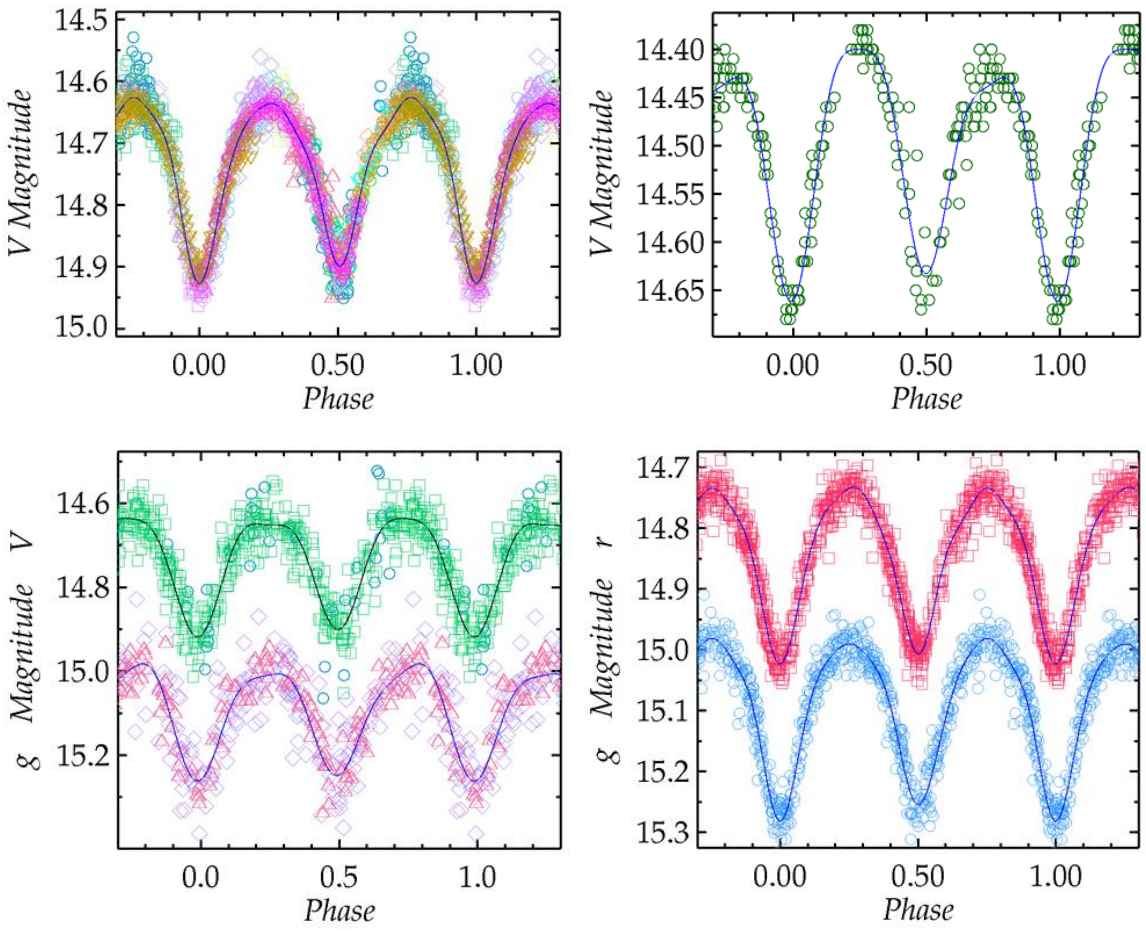

Figure 11: The phase diagrams of different data sets of GSC 03465-00810 folded on the ephemeris in Equation 3, where the times have been corrected for the LTTE as shown in Figure 10. (Top left) All the time-series data where different symbols indicate different runs. (Top right) The CSS V -band data. (Bottom left) The ASAS-SN V - and g-band data with different cameras identified. (Bottom right) The ZTF g and r data, with the r data offset by -$0^m.25$ from the g data. All the other bands are shown at the correct level.

prospect for eclipse timings, both individually from the time-series data and as composite timings from the synoptic projects. The O–C diagram is shown in Figure 10 and there is a clear variation in the residuals of $\sim\pm 0^{d}.01$, which is typical of third bodies in low-mass systems. The line shows the light-travel-time effect solution, but it is not completely clear cut. The third-body period is probably $\sim$4000 d, but longer-period solutions are possible although they are driven to higher eccentricities and larger amplitudes of the LTTE, which generate increasingly unrealistic masses for the system. With $P_3 \sim$ 4000 d the minimum mass of the third body is $\sim 0.5\ M_{\odot}$ and may make a significant contribution to the luminosity of the system, which – limited data suggest – may be about half a magnitude brighter than other W UMa systems of a similar period. So, there is some headroom in the luminosity for a third light contribution. A detailed description of the system has been published elsewhere [15]. The ephemeris of primary minimum is

$$HJD_{\mathrm{MinI}} = 2454172.6607(6) + 0.27668359(4) \times E \qquad (3)$$

and the O–C residuals should continue to reduce for a few years before the period starts increasing again.

References

1. I. Miller, *British Astronomical Association Variable Star Section Circular*, **134**, 22 (2007)
2. B. J. Shappee, et al., *ApJ*, **788**, 48 (2014)
3. C. S. Kochanek, et al., *PASP*, **129**, 104502 (2017)
4. J. L. Tonry, et al., *PASP*, **130**, 064505 (2018)
5. K. W. Smith, et al., *PASP*, **132**, 085002 (2020)
6. F. J. Masci, et al., *PASP*, **131**, 018003 (2019)
7. X. Chen, et al., *ApJ Suppl*, **249**, 18 (2020)
8. I. Miller, *British Astronomical Association Variable Star Section Circular*, **170**, 8 (2016)
9. G. R. Ricker, et al., *Journal of Astronomical Telescopes, Instruments, and Systems*, **1**, 014003 (2015)
10. T. Jayasinghe, et al., *MNRAS*, **493**, 4045 (2020)
11. R. P. Kraft, *ApJ*, **150**, 551 (1967)
12. M. Xiang, et al., *ApJ Suppl*, **245**, 34 (2019)
13. C. Lloyd, I. Miller, *Open European Journal on Variable Stars*, **237**, 1 (2023)
14. I. Miller, *British Astronomical Association Variable Star Section Circular*, **175**, 21 (2018)
15. C. Lloyd, et al., *The Observatory*, **141**, 223 (2021)

A personal project to observe some neglected SR and L variables. 1

Don Mathews

don@mountainsandwildlife.co.uk

Over the last few years, I have undertaken a personal project to observe some SR and L type variables, mostly with few or no observations in the BAA or AAVSO databases, using a telescope / DSLR combination and ensemble photometry of the images. This has demonstrated that it is quite practicable to generate one's own comparison star sequences from APASS and Tycho2 data. For SR and L variables with small ranges of variation, photometric observation can give more consistent results than visual observing, where eyesight differences between individuals can be significant. VStar period analyses of my observations have been undertaken by Shaun Albrighton and the results are included in this summary. All observations resulting from this personal project have been added to the BAA database.

Introduction

Back in the winter of 2017/18 I started a personal project to look at some semi-regular and long period variables in the AAVSO's Variable Star Index (VSX) that have few, or in many cases no, observations recorded in either the BAA or AAVSO databases. SR and L variables tend to be more neglected than Miras are more amenable to photometric monitoring than to visual observing, the variations between instruments being around an order of magnitude smaller than those between human eyes for stars with high B-Vs (pers. obs.).

My kit, comprising a V-filtered Nikon DSLR attached to a 203mm Celestron SCT, works best between magnitudes 10 and 14. In this range, I can also use the AAVSO's APASS star catalogue to establish appropriate comparison star sequences for the ensemble photometry where no standard sequences are available, though for some variables that turned out to be slightly brighter than expected it was necessary to turn to the Tycho2 catalogue, with magnitudes converted from Vt to V.

Living to the north of an urban / industrial area, the northern half of my sky is better for astronomy than that to the south. My project therefore chose stars with declinations north of 55°N, which has the added advantage of ensuring that they stay high enough in the sky for effective photography throughout the year (always more than about 20° above the horizon at my latitude). The first constellations to be reviewed for suitable variables were Ursa Major and Ursa Minor, with some stars in Camelopardalis added in August 2018. The UMa/UMi part of the project was partially wound down in mid-2020 and the remainder (with one exception) terminated in mid-2022. The one exception is RZ UMa, which is in the BAAVSS Pulsating Star Programme and continues to be monitored.

Broad Conclusions

1. The project proved worthwhile in that it established that for some poorly observed variables a personal study of this nature has the potential to augment, and in a few cases challenge, the characteristics listed in VSX.
2. As expected, the range of magnitude variation for many of these SR and L stars is better suited to photometric than visual observing.

3. Where no comparison star sequence exists, creating one's own from APASS data is practicable but requires a little care as some stars in the APASS catalogue can exhibit a small degree of variability and need to be excluded from the photometric sequence.

Methodology

Observations were undertaken with a Nikon DSLR (mainly a D7500 model) fitted with a V filter and attached to a 203mm Celestron SCT. The camera was not astro-modified and all three colours were used, reliance being placed on the V filter to give a reasonable measure of the star's brightness. Twenty images were usually taken, with exposures of between 0.5 and 20 seconds to match the expected magnitude of the variable. Images were pre-processed and stacked using IRIS and ensemble photometry of the stacked image undertaken with Astroart6. The resulting magnitudes were submitted to the BAA database.

For some of the stars in this project, comparison star sequences can be accessed via the AAVSO Variable Star Plotter [1], telescopic (1°) sequences being available for BI Cam, HX Cam, RX UMa, RZ UMa, TZ UMa and WW UMa. However, most comparison star sequences for this project were established using magnitudes from the APASS catalogue [2]. In the early part of an observing campaign, a large number of comparison stars were used for each variable (typically around ten or twelve) and the errors given in the Astroart6 photometry results were tabulated and reviewed. Any stars showing significant errors, either consistent or erratic, were then excluded and the photometry repeated. Finally, a set of between four and six stars spanning the expected range of the variable was established as the comparison sequence and all photometry was undertaken on this consistent basis. For a few variables that proved to be slightly brighter than magnitude 10, a similar process was undertaken using Tycho2 data taken from the European Space Agency's ESASky website [3]. In this case V magnitudes were calculated from the Vt and Bt values using the V=Vt-0.09(Bt-Vt) relationship given in the NASA website [4].

Period analyses of the results of this project have been undertaken by Shaun Albrighton, BAAVSS Pulsating Stars Co-ordinator, using the AAVSO's VStar program [5]. However, any errors of interpretation are solely the responsibility of the author.

References

1. AAVSO Variable Star Plotter: https://app.aavso.org/vsp/
2. AAVSO APASS data download: https://www.aavso.org/download-apass-data
3. European Space Agency ESASky: https://sky.esa.int/esasky/
4. NASA HEASARC archive: https://heasarc.gsfc.nasa.gov/W3Browse/all/tycho2.html
5. AAVSO VStar program: https://www.aavso.org/vstar

Results

Camelopardalis

BG Cam:
Current information: VSX: LB; 11.38 - 11.81 V; 350d
No observations in the BAA or AAVSO databases prior to this study. Nine more recent V observations in the AAVSO database.
Project results: The range of this star is larger than the published one, with my observations being between 11.4 and 12.7 V. On data gathered between October 2018 and March 2022, the period appears to be longer than 350 days. VStar analysis suggested a period of 545 days but observations over a longer period of time would be needed to confirm this.
Type appears to be SR; observed V range was 11.4 - 12.7 V; period appears to be >350d; further observations would be beneficial.

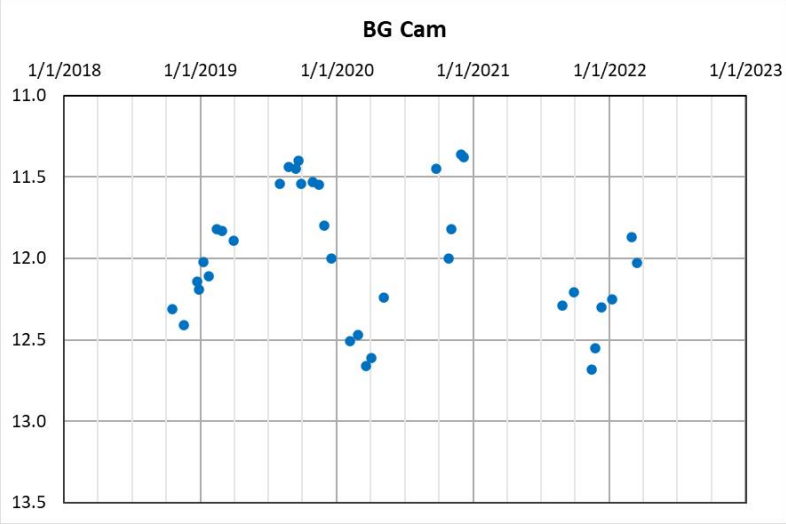

BI Cam:

Current information: VSX: LB; 8.2 - 9.0 R
No observations in the BAA or AAVSO databases.
Project results: Observations between September 2018 and March 2022 ranged between 10.6 and 11.3 V, with no obvious periodicity. VStar also found no obvious period.
Observed V range was 10.6 - 11.3V

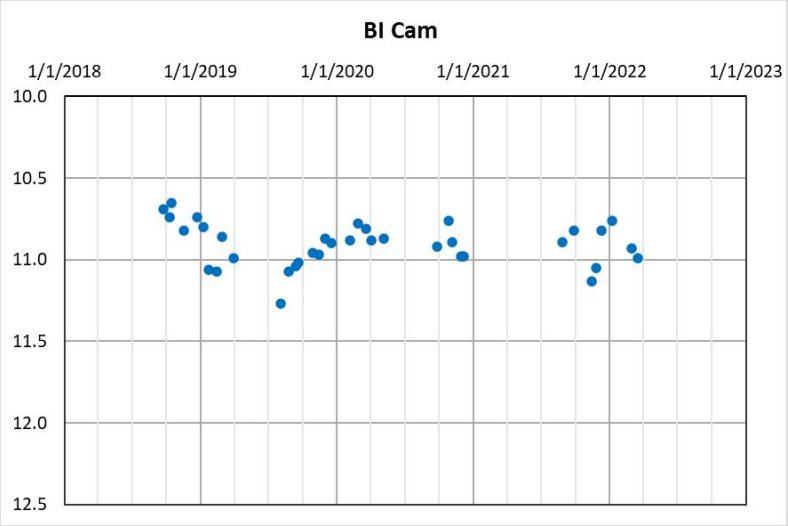

FZ Cam:
Current information: VSX: SR; 12.1 - 13.2 V; 124.7156194 d
No observations in the BAA or AAVSO databases.
Project results: My observed range of 11.8 to 13.0 V is very similar to the published one, though very slightly brighter. An apparent period in the region of 4 months was confirmed by VStar at 121 days, very close to the c.125 days in the 2020 VSX update.
Observed V range was 11.8 - 13.0 V.

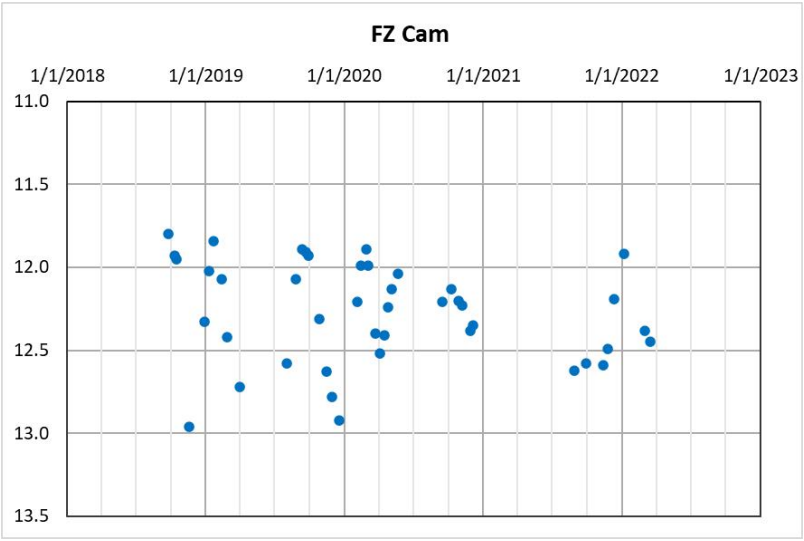

GK Cam:

Current information: VSX: SR; 12.1 - 12.9 V; 131d
No observations in the BAA or AAVSO databases.
Project results: Observations between September 2018 and March 2022 ranged between 12.5 and 13.9 V, a slightly wider and overall, somewhat fainter range than the published one. VStar gave a period of 148 days, a little longer than the published 131 day figure.
Observed V range was 12.5 - 13.9 V; period appears to be 148d.

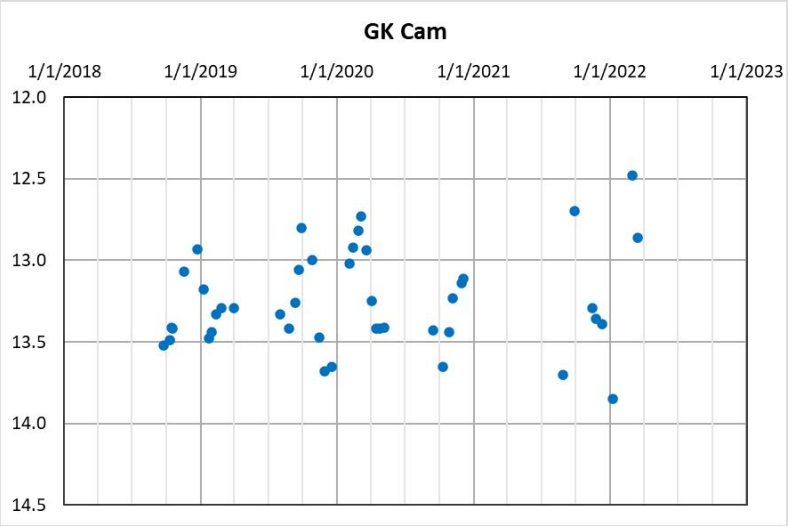

GW Cam:

Current information: VSX: SRB; 12.2 - 13.0 V; 79d
No observations in the BAA or AAVSO databases.
Project results: Observations between September 2018 and March 2022 ranged between 12.4 and 13.3 V, a little fainter than the published range. The observed period appears to be a little shorter than the published 79 days; VStar gave a figure of around 64 days.
Observed V range was 12.4 - 13.3 V; period appears to be <79d.

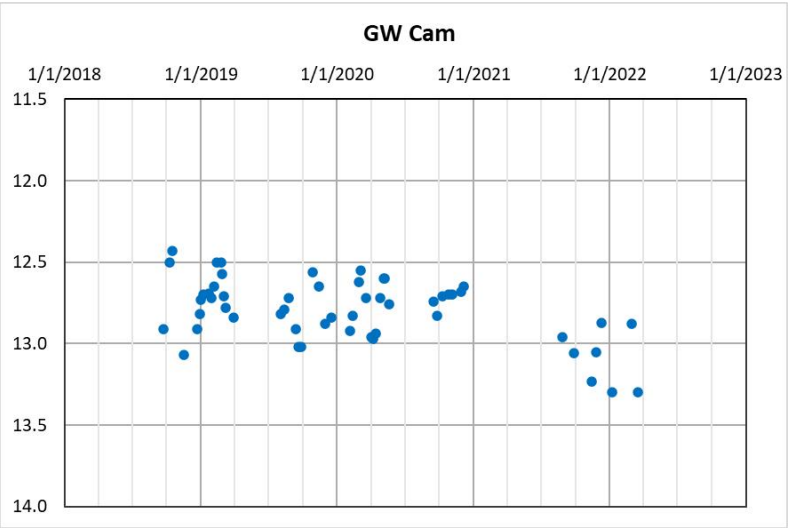

HX Cam:
Current information: VSX: SR; 12.7 - 13.2 V
No observations in the BAA or AAVSO databases.
Project results: Observations between September 2018 and March 2022 ranged between 13.0 and 13.8 V and were mainly fainter than the published range. There appeared to be a period somewhere in the 4-month to 6-month range. VStar gave a primary period of 186 days, at the long end of this range, with a possible secondary period of around one year, though this might be an artefact as it is about double the primary period.
Observed V range was 13.0 - 13.8 V; possible period of 186 days.

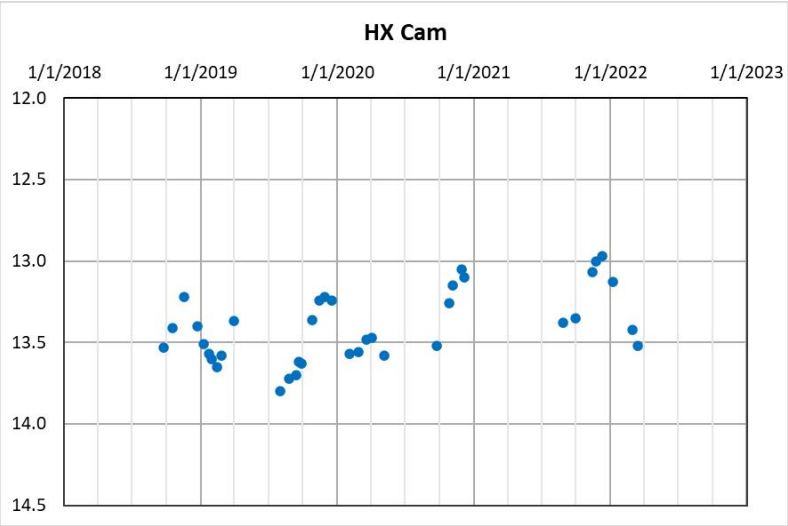

IT Cam:
Current information: VSX: SRB; 12.1 - 12.8 V; 133d
No observations in the BAA database; 2 V observations in the AAVSO database.
Project results: Observations between September 2018 and December 2020 varied between 12.5 and 13.5 V, mostly below the lower limit of the published range, but had jumped to 12.0 when observations were restarted in August 2021. VStar gave a period of 137 days, very close to the published figure.
Observed V range was 12.0 - 13.5 V.

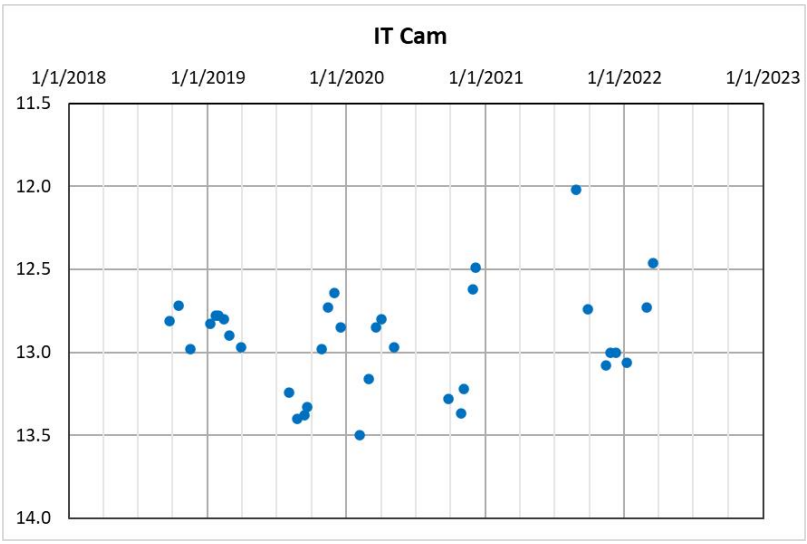

IV Cam:
Current information: VSX: SR; 11.4 - 12.4 V
No observations in the BAA or AAVSO databases.
Project results: Between September 2018 and March 2022 all observations were between 11.5 and 12.4 V, within the published range. There was an indication of a period of around 3 months and VStar confirmed this with a period of 89 days.
Possible period of 89 days

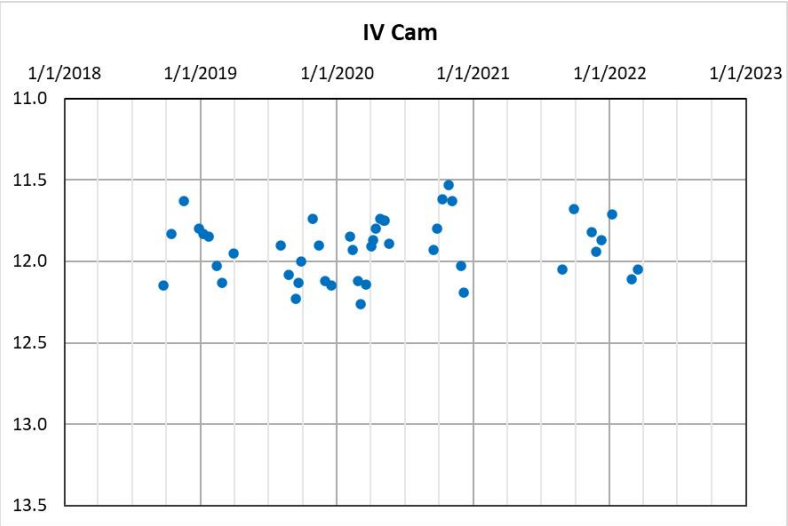

KL Cam:
Current information: VSX: SR; 10.8 - 12.9 V; 170d
No observations in the BAA or AAVSO databases
Project results: All observations between September 2018 and March 2022 were between 10.7 and 12.1 V, compatible with the brighter end of the published range. Observations in 2019-20 were suggestive of a period significantly shorter than the published 170 days, possibly at about half this period, but at other times 170 days looked reasonable. VStar gave a somewhat different picture, with a clear period of 194 days but also with weaker periods of 95 days and 158 days. The situation is not clear and further observations would be beneficial.

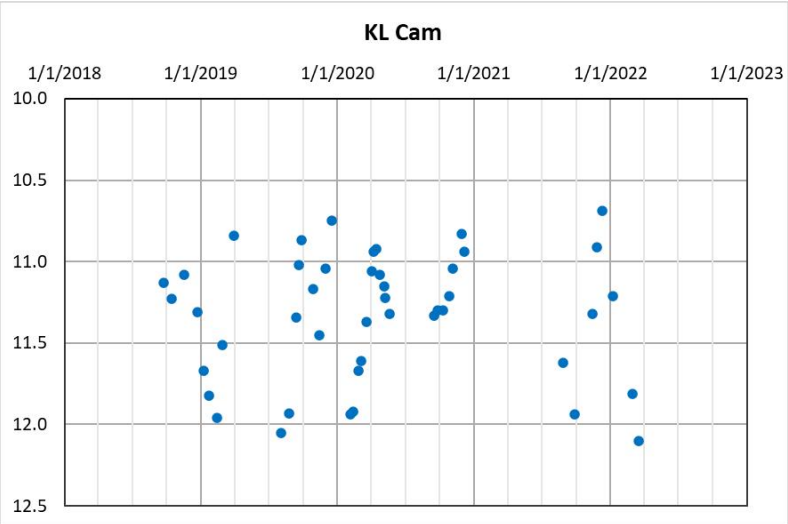

KW Cam:
Current information: VSX: SR; 10.3 - 11.4 V; 125d
No observations in the BAA or AAVSO databases.
Project results: Between September 2018 and March 2022 all observations were between 10.6 and 11.7 V, broadly compatible with the published range. There was no obvious period visible in the early observations but a greater variability appeared subsequently, with minima in September 2019, December 2019 and March 2020 only about 90 days apart. VStar hinted at possible periods of 89 days and 161 days.
Observed V range was 10.6 - 11.7 V; further observations would be beneficial.

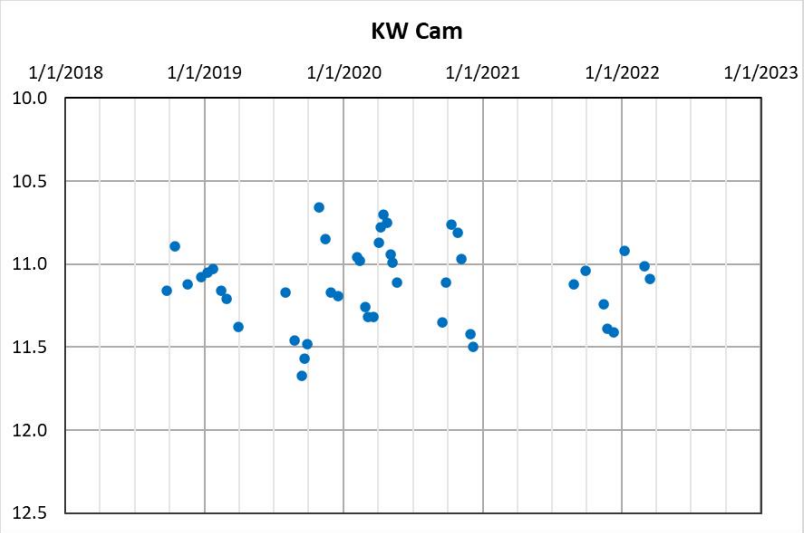

Pseudo-Periodicity in OJ287 in 2023?

Mark Kidger
cricketingstargazer@gmail.com

Periodicity analysis is a powerful tool to analyse astrophysical processes. Of course, many types of periodicity exist in the world of variable stars: pulsational, vibrational, rotational, and orbital. Analysis of these periodic signals gives us valuable information about the body that is producing them. It is now accepted that periodicity is not a significant element of quasar light curves, although a long and sometimes bitter debate raged about it for two decades from the 1960s to 1980s. However, there are many cases of what appeared to be short-term periodic signals in quasar light curves. Such pseudo-periodicities have been largely ignored but carry potentially valuable information. During the second half of the winter 2022/23 observing campaign, there are suggestions of possible pseudo-periodicity of 6.71±0.01 days in OJ287, an object long suspected of showing epochs of apparent pseudo-periodicity.

Periodicity v pseudo-periodicity

What do we mean by pseudo-periodicity? Periodicity is a repeated signal that appears or reproduces at a set interval. Examples are Cepheid variables, pulsars, Algol type variables, RS CVn stars, etc. You can predict the behaviour of the star weeks, months, or years ahead because the signal repeats in an exactly predictable fashion because there is an underlying astrophysical process happening in a regular pattern. This may be the oscillation of a star, the rotation of two stars about their common centre of gravity, or the rotation of a star that reveals and hides massive starspots. In contrast, pseudo-periodicity is an apparently periodic variation that appears and disappears at random moments and, usually, does not repeat. It also has little or no predictive power other than short-term. In other words, a pseudo-periodicity is a temporary, unstable period. As such, it is frustrating for the observer because just when you think that you are seeing what appears to be a stable, cyclic variation, it disappears. You can never be certain that it is a genuine signal, or just a result of random variations that seem to stabilise briefly, mimicking periodicity. For this reason, unless there are multiple cycles of the variation, it is not reasonable to claim that there is even a temporary periodic signal.

Periodicity v random behaviour in quasar light curves

Quasars were discovered sixty years ago. It is accepted now that quasar light curves are essentially random in nature. In other words, periodicity is not the key to their variations. During the 1960s, ‘70s and ‘80s there were multiple cases of periodicity analysis of quasar light curves and many claims of periodic behaviour. Often the claimed “period” was based on a data sample little longer than the light curve itself. Two of the earliest and best-documented cases concerned 3C273 and 3C345.

3C273: It was realised immediately that, because of its brightness (magnitude 13), hundreds of pre-discovery images exist in the Harvard plate collection. This allowed a light curve to be built up from 1885. Attention focussed rapidly on a particularly well-covered epoch in the 1920s and ‘30s that showed what appeared to be a perfect sinusoidal variation of period 13 years. A frequently heated debate built up between groups who found a stable 13-year period through the full light curve (e.g., Ozernoy, Gudzenko & Chertoprud, 1977) and those that believed this sinusoid to be a single, random event and that the light curve was dominated by random processes (e.g., Fahlman & Ulrich, 1976).

3C345: This object was recognised in 1965. A three-year light curve study by Tom Kinman and colleagues at Lick Observatory (Kinman et al., 1968) showed regular flares every 80 days. What was particularly interesting was that the amplitude of the flares was remarkably constant even though the base level of the light curve varied considerably. Over the course of their study, they observed nine of these regular flares. Kinman et al. waited until they were certain of the periodicity before publishing: of course, the 80-day cycle disappeared even before the paper appeared!

A similar case occurred with a putative 1500 day cycle in large outbursts of this quasar. Three, large outbursts, the first of which was reported by Kinman et al., were observed over an interval of eight years, in 1968, 1972 and 1976 and reported by Barbieri et al. (1977) and re-iterated in later papers. The predicted 1980 outburst did not appear and, although a new outburst did occur in 1984, it did not agree with the expected timing from the previous outbursts. Although period searches continued to show this 1500-day signal in the extended light curve, it was merely a reflection of these three, equally spaced outbursts in an early part of the global light curve and, in no sense, a real or enduring periodicity within the full dataset (e.g., Kidger, 1989).

By the end of the 1980s, the possible existence of long-term periodicity in quasars was discredited save for the case of the 11.8 year period in the outbursts of OJ287 (e.g., Valtonen et al., 2023), although multiple models have been proposed to explain the outbursts.

My own attention was particularly directed at OJ287 due to the many reports of rapid periodicity in the light curve. Many such reports were made in the 1970s and '80s, both in the visible and in radio data, almost always with reported periods around 20 and 40 minutes (e.g., Valtaoja et al., 1985 and references therein). Typical amplitudes of variation were 1-2%. However, despite the multiplicity of reports, no period was ever firmly confirmed independently and, indeed, study of near-simultaneous data from different observatories reached different conclusions as to the existence of the reported period. As later pointed out (Lehto, 1994) the period observed by Valtaoja et al. (1985) appeared and disappeared again several times throughout several months of monitoring so, once again, appears to have been a pseudo-periodicity rather than a genuine periodicity. Even so, such activity has great potential astrophysical interest as it could, for example, mark the period of the innermost stable orbit around the central black hole, thus giving a clue as to the mass of the singularity, or be linked to some similar process within the quasar.

2022-23 campaign data

An initial report on the campaign was made in the March BAA-VSS Circular. Unfortunately, the date of the predicted 2022 outburst was exactly centred on solar conjunction. Campaign data only served to confirm that an alternative prediction that gave a potential peak of outburst as much as four months later was invalid. Monitoring reported by Valtonen et al. (2023) constrains the epoch of the (unobserved) outburst very tightly, with photometry in early July (a month later than the latest available data from amateur monitoring) and in late August (a month earlier than the earliest data reported here) showing no trace of an outburst.

As can be seen in Figure 1, the light curve is very active, but it should be noted that OJ287 has faded about 2 magnitudes from the level that it had in late 2015 (Figure 2) and the 2022-23 campaign has been marked with several epochs when OJ287 became as faint as V~16.5, an unusually low level in this object.

An issue that must be faced is that data is, inevitably, reported in many photometric systems. Although Star 4 of the standard sequence (Penston & Wing, 1973) is used as reference, there are inevitable differences if the data is obtained in white light, with a standard Johnson-Kron-Cousins V filter, or in sG or Gaia G. Similarly, due to the red colour of the continuum, the use of blue-sensitive or red-sensitive CCD chip also significantly affects the photometry. Here, it is assumed that the colour

index of OJ287 is constant, and that photometry can be transformed by a simple zero-point correction.

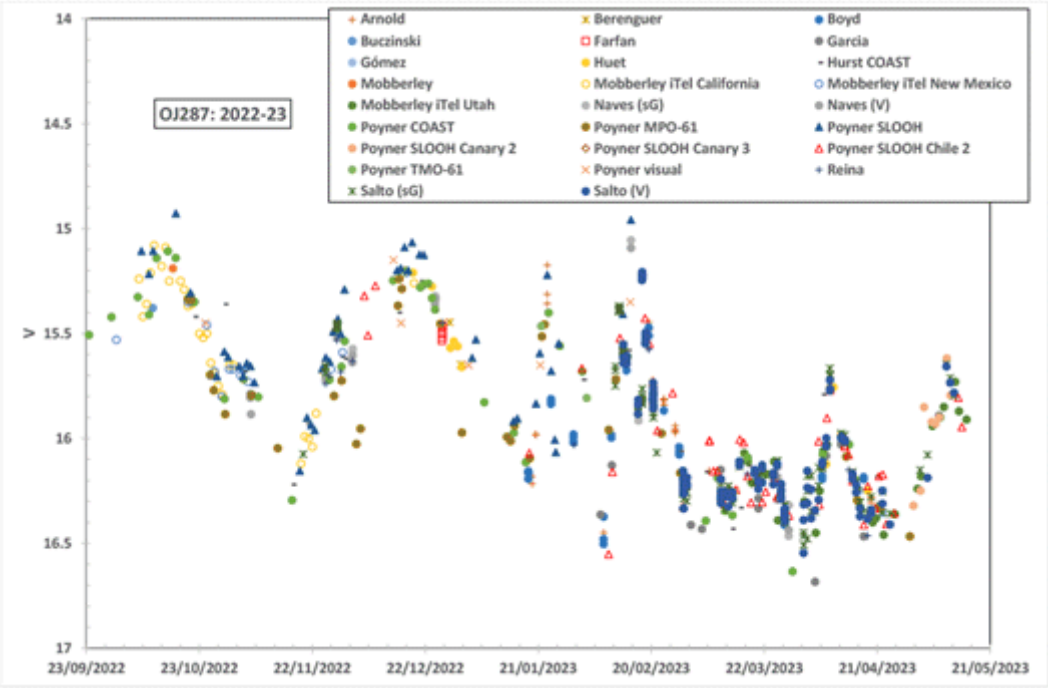

Figure 1: OJ287 light curve data for the 2022-23 campaign. This included all reported data in the V, G, sG and CV systems, each of which has been transformed to a consistent zero-point in V.

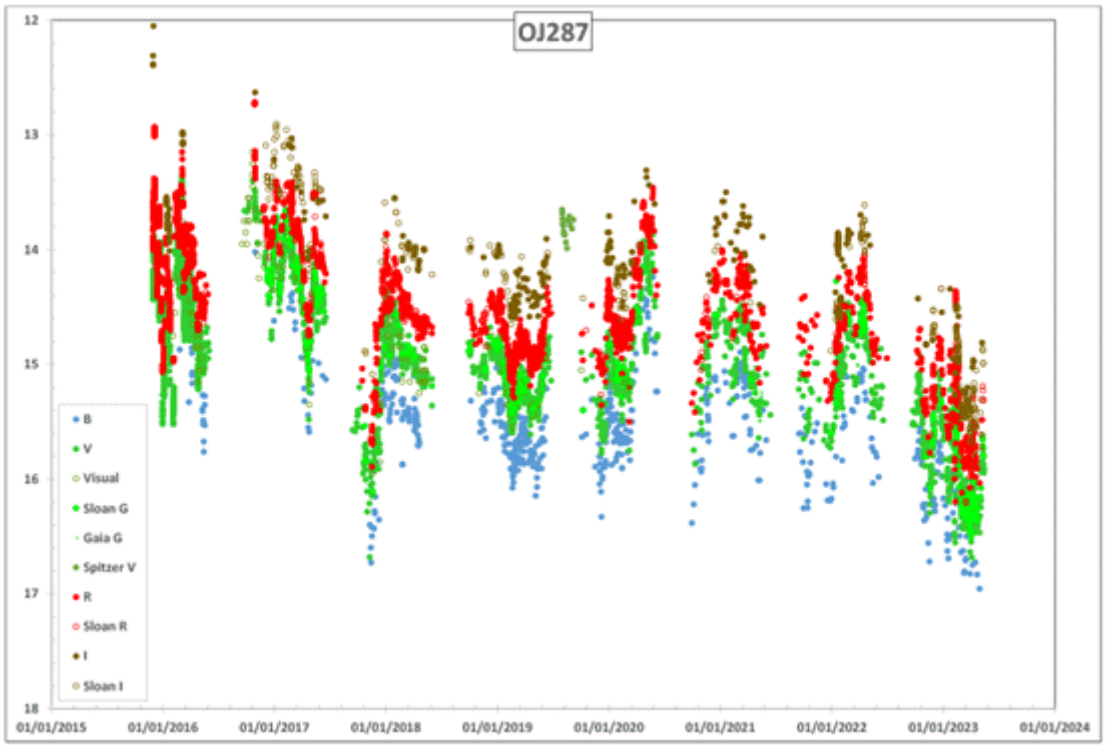

Figure 2: Full campaign data since 2015 in B, V, R and I. Data reported as sR and sI have been transformed to a consistent zero-point with broadband R and I photometry in the same way as in Figure 1.

Where sufficient data exists for an observer, the zero-point correction is determined empirically by applying different corrections and testing which reduced most the residuals with the rest of the ensemble of data. As a result, after zero-point correction and transformation, we have:

- 79 observations in B
- 774 observations in V
- 440 observations in R
- 181 observations in I

Period analysis methods

As the V-band light curve is by some distance the best sampled, this analysis concentrates on this band. In Figure 1, it is evident that there is a change in behaviour from the slow variations of timescale ~2 months and amplitude ~1 magnitude that were seen between September 2022 and mid-January 2023 to the much faster variations seen from mid-January 2013. Visual inspection of the light curve suggested that peaks tended to happen at intervals of ~6 days, although not all expected peaks do appear. What was less clear was that this a genuine feature of the light curve, or simply a false visual association in which the eye sees non-existent patterns in data.

To investigate the characteristics of the light curve, Peranso analysis was used, using version 3.0.4.0 (Paunzen & Vanmunster, 2016). Peranso is an extremely powerful tool that offers many different methods of periodicity analysis. In general, they divide into two basic types:

- Fourier analysis using decomposition of the light curve into the combination of sine waves of different amplitude and
- Periodogram analysis in which the light curve is folded over many test periods and the period or periods that minimise the dispersion in the folded data are selected.

The former is the classical analysis used in many branches of astrophysics, while the latter is a powerful tool when the signal that is being searched for cannot be simply decomposed into a sine wave, or into a simple combination of sine waves (e.g., planetary transits, or Algol type variables).

The choice of method of analysis tends to be a matter of personal preference. Initial studies in the 1960s and ’70 relied on modifying quasar light curve data to make it equally spaced and revealed that the way in which data was pre-processed greatly affected the results. This changed with the introduction of Deeming analysis, which provided a powerful method of analysing unequally-spaced data (Deeming, 1975), revolutionised light curve analysis and is still a popular tool. Many variants of Deeming analysis have since been developed for particular types of data: for example, the CLEANest algorithm (Foster, 1989) was developed for the cases in which multiple periods are present, some of which are spurious ones due to sampling. Other methods such as Lomb-Scargle (Scargle, 1981) are optimised for searching for periodic signals in noisy data. This last method has under multiple refinements over the years culminating in a generalised form of the algorithm that applied Baysian analysis to data from photon-counting systems (Scargle, 1998).

However, there are two basic tenets that apply to period analysis:

- If different methods of analysis give different results, the period is almost certainly not genuine.
- Unless the period is of very low amplitude and thus more suitable for analysis using the Lomb-Scargle algorithm, there should be evidence of it in the raw light curve before analysis. In other words, “ask and it shall be given, seek and you shall find” – be suspicious of periods found in noisy data that are not evident to visual inspection of the light curve!

Here, three principal methods suited to the dataset are used (Deeming, CLEANest and Jurkevich), with other methods used as a cross-check of results.

Analysis

The dataset is split into two sets: a full data set consisting of 757 observations obtained between 2022 September 22 and 2023 May 15 and a more limited data set consisting of 550 observations obtained between 2023 January 14 and May 15 in which the potential periodic signal is most obvious in the form of a series of rapid, short-lived flares. Given that there is a strong fading trend during the observing season, the data was de-trended using a linear regression and normalised to the mean level. No other pre-treatment was applied to the data. Periods were searched for in the range 2.5 to 40 days. A search for shorter periods makes no sense when the data is dominated by daily sampling and is obtained from a limited range of longitudes between 0° and 110° West, while periods longer than 40 days are too severely unsampled in the data.

A problem in periodicity analysis is that of spurious periods due to periodic patterns in sampling. Fewer observations are made at Full Moon and when the Moon is closest to the target being observed. Subtler effects may also be present, such as an increased tendency to observe, for example, at weekends. While CCD detectors have reduced the tendency to observe a spurious period of 29.5 days in light curves (the interval between Full Moons), the fact that OJ287 is in the Ecliptic and that the Moon passes very close each sidereal month means that there will always be a strong, spurious signal around a period of 27.3 days. This effect can be quantified by generating the spectral window – effectively a map of spurious periods caused by sampling (Figure 3). As expected, we see a strong spurious period at close to one sidereal month. We see weaker periods, apparently harmonics, at around one half and one third of a sidereal month.

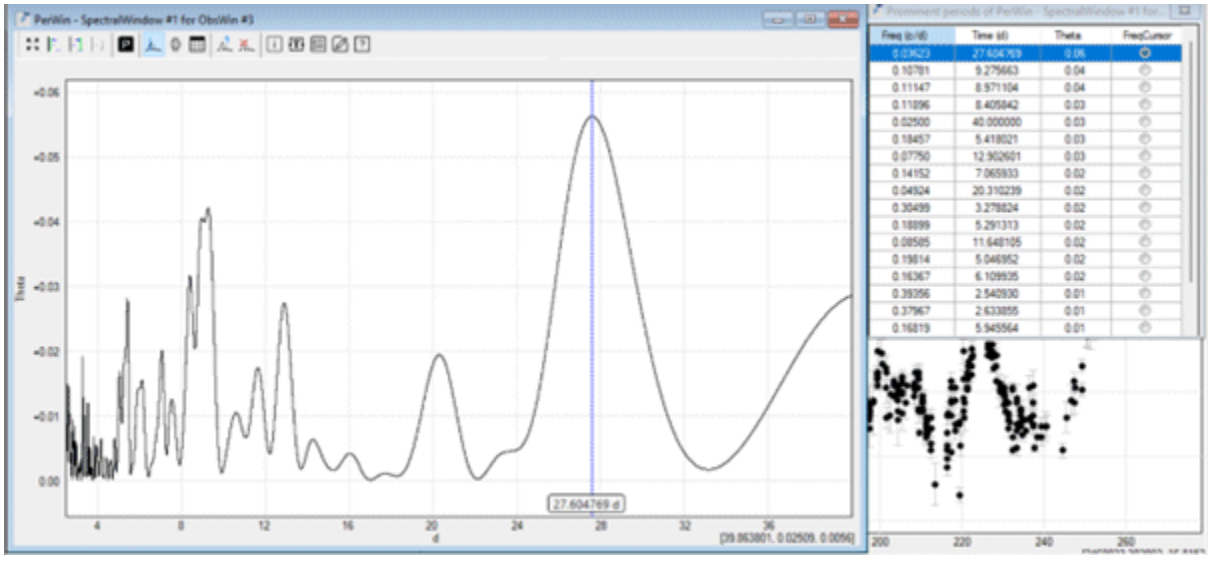

Figure 3: The spectral window for observations of OJ287 during the 2022-23 campaign. The main spurious period is identified in the graphical representation (left), while the table (right) lists the main periods that are detected. A strong signal is detected, as expected, close to one sidereal month.

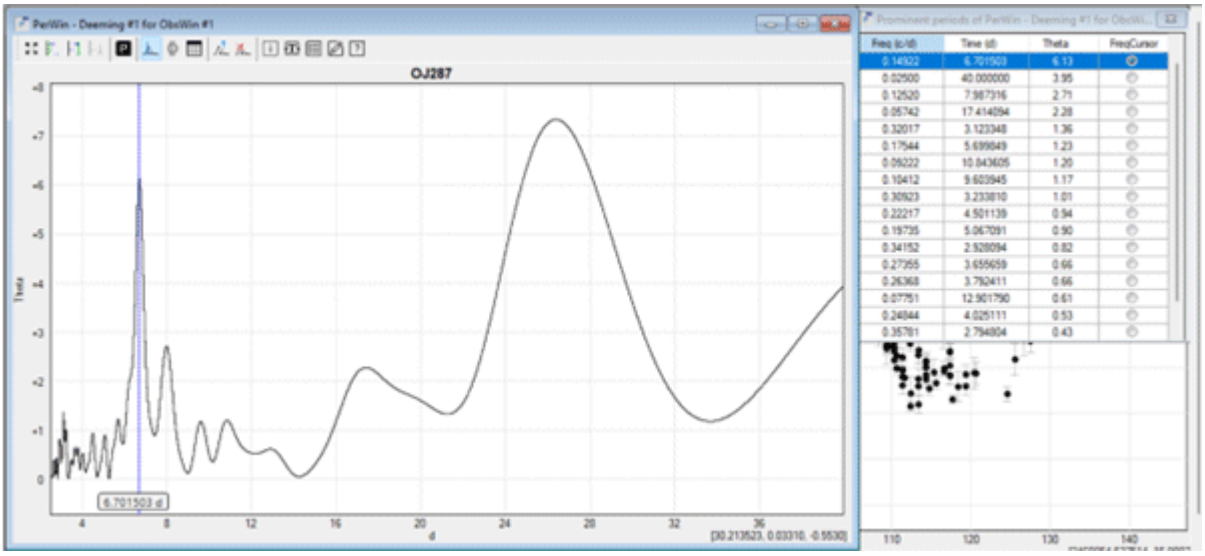

Figure 4: Deeming analysis of the reduced data set. Apart from the spurious period at a sidereal month, a strong signal is seen at a period of 6.70 days. There is no period in the spectral window that corresponds to this signal, thus it is probably intrinsic to the light curve.

Deeming analysis of the reduced dataset gives the result shown in Figure 4. Apart from the spurious period caused by sampling, at one sidereal month there is a strong periodic signal revealed by the peak at 6.70 days that does not appear in the spectral window. This peak is sharp, suggesting that it is well-defined. The same data set was analysed using the CLEANest algorithm, with almost identical results (Figure 5). The main differences are that the period is fractionally longer (6.72 days, instead of 6.70) and the sidereal sampling peak is slightly shifted to shorter period.

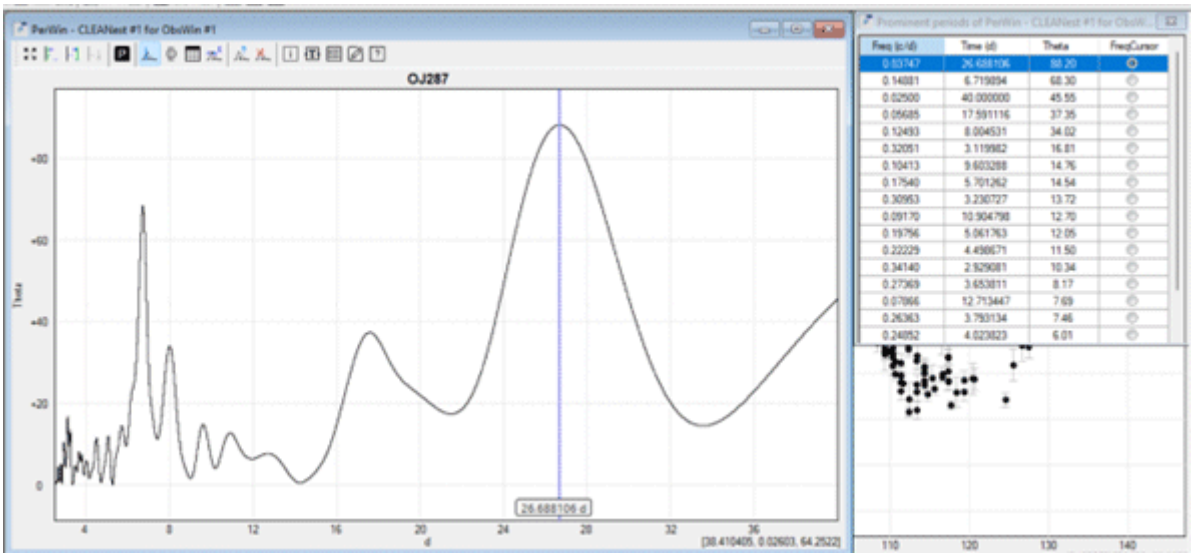

Figure 5: CLEANest analysis of the same reduced data set as Figure 4. Very similar results are seen, with a strong period indicated at 6.72 days.

Finally, we show the Jurkevich analysis (Figure 6). The advantage of this method is that it is insensitive to the shape of potential periodic variations. As it uses a completely different method to the previous two, we would expect differences of detail. The spurious signal at a sidereal month breaks into multiple peaks due to random alignments of data around this spurious sampling period. Again, though, we see a strong signal around 6.7 days – in this case, 6.72 days again – although there is also a signal at 6.87 days that is probably due to random groupings of phased data causing alternative best fits.

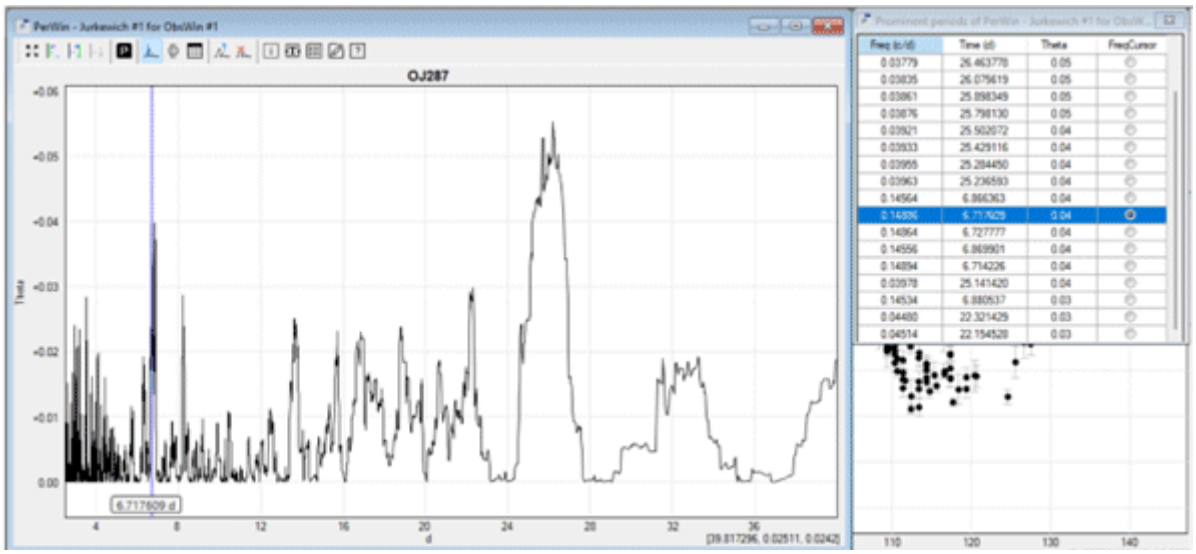

Figure 6: Jurkevich analysis of the same reduced data set as Figure 4. Similar results are seen, with a strong period indicated at 6.72 days and another period at 6.87 days that is not seen in other analyses.

Peranso allows the light curve to be folded around any period in the period table displayed, fitting a mean light curve to the period. The result, for 6.72 days, is shown in Figure 7.

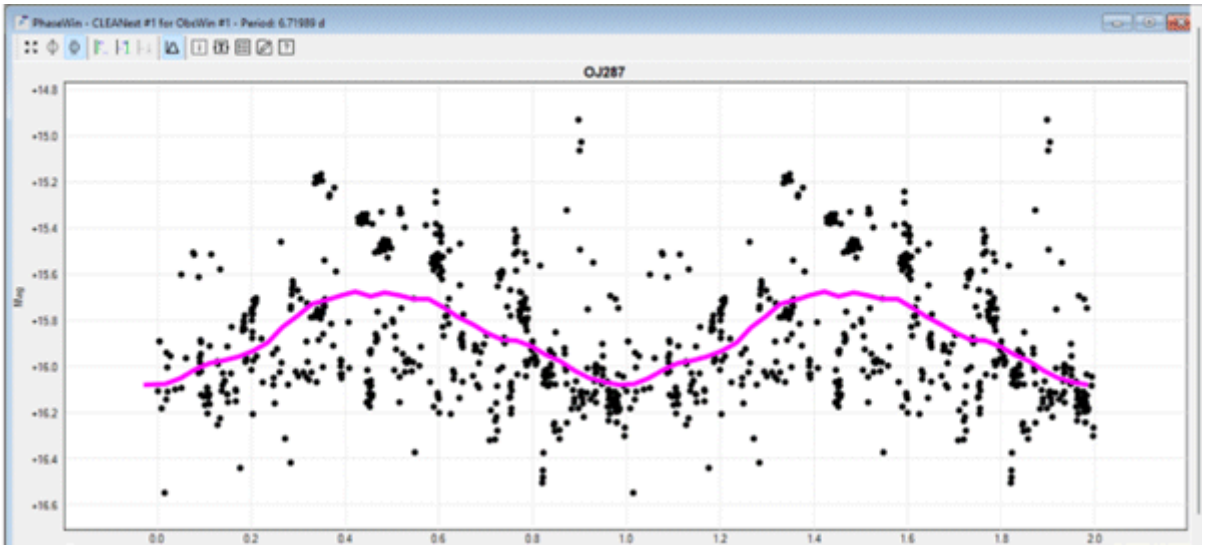

Figure 7: The light curve for the reduced data set folded around a period of 6.72 days, with the mean light curve fitted. The fit seems plausible and does not appear to be due to random alignments of data causing a spurious result. The mean amplitude is 0.4 magnitudes.

Similar results are found in all analyses with other suitable algorithms tested in Peranso (Bloomfield, 6.74d; Lomb-Scargle, 6.72d; FALC, 6.71d), thus there seems to be reason to believe that this may be a genuine signal from the quasar. We would not expect to see this period in the first half of the data set in which there is no evidence for it on visual inspection so, this part of the data should act as a control sample. This is effectively what we find: no signal is seen in the data at 6.7±0.2 days.

Discussion

There is a long history of reports of apparent periodic behaviour in quasars that have never been confirmed, thus all such reports should be treated with great caution. However, the potential 6.71±0.01 day period in flaring activity has endured now for 4 months and, although it is clearly not a genuine periodicity, there is increasing evidence that it may not be completely spurious and may indicate some temporary physical process within the quasar.

Flares are believed to be generated in the relativistic jets of blazars and to be caused by shocks within the jet. A potential explanation for such a pattern in flares would be similar to the most likely explanation for the periodic flaring in 3C345 in 1965-68: a lighthouse effect. In other words, something is crossing our line of sight every 6.71 days. If a shock is spiralling around the magnetic field of the jet, we would expect to see a flash each time it aligns itself most closely with our line of sight, in a similar way to seeing a flash when a lighthouse beam or a pulsar's beam points towards us. The pseudo-periodicity would last only as long as the shock continues to cross our line of sight.

Acknowledgement

This research made use of Peranso (www.peranso.com), a light curve and period analysis software.

I would like to thank all the observers (see Figure 1 for the names of all observers who have contributed data) for their continuing efforts.

References

Barbieri, C. ; Romano, G. ; di Serego, S. ; Zambon, M., 1977, Survey of the optical variability of compact extragalactic objects. I. The field of 3C 345, Astronomy and Astrophysics, 59, 419

Deeming, T. J., Fourier Analysis with Unequally Spaced Data, Astrophysics and Space Science, 36, 137

Fahlman, G. G. ; Ulrych, Tad J., 1976, Shot Noise in 3c 273, Astrophysical Journal, 209, 663

Foster, G., 1995, The Cleanest Fourier Spectrum, Astronomical Journal 109, 1889

Kidger, M. R., 1989, The optical variability of 3C 345, Astronomy and Astrophysics, 226, 9

Kinman, T. D. ; Lamla, E. ; Ciurla, T. ; Harlan, E. ; Wirtanen, C. A., 1968, The Variability of the Optical Brightness and Polarization of the Quasistellar Radio Source 3c 345, Astrophysical Journal, 152, 357

Lehto, H.J., 1984, Private communication

Ozernoi, L. M. ; Gudzenko, L. I. ; Chertoprud, V. E., 1977, Comments on the light curve of the quasar 3C 273, Astrophysical Journal, 216, 237

Paunzen, E. & Vanmunster, T., 2016, Peranso - Light Curve and Period Analysis Software. Astronomische Nachrichten 337, 239

Penston, M. V. & Wing, R. F., 1973, A photoelectric sequence in the field of OJ 287, The Observatory, 93, 149

Scargle, J. D., 1981, Studies in astronomical time series analysis. I - Modeling random processes in the time domain, Astrophysical Journal Supplement Series, 45, 1

Scargle, J.D., 1998, Studies in Astronomical Time Series Analysis. V. Bayesian Blocks, a New Method to Analyze Structure in Photon Counting Data, The Astrophysical Journal, 504, 405

Valtaoja, E., Lehto, H., Teerikorpi, P., Korhonen, T., Valtonen, M., Teräsranta, H., Salonen, E., Urpo, S., Tiuri, M., Piirola, V., Saslaw, W. C., 1985, A 15.7-min periodicity in OJ287, Nature, 314, 148

Valtonen, M.J. et al., 2023, Refining the OJ 287 2022 impact flare arrival epoch, Monthly Notices of the Royal Astronomical Society, 521, 6143

Eclipsing Binary News

Des Loughney

desloughney@blueyonder.co.uk

Record Breaking Eclipsing Binary: TYC-2505-672-1

A team of scientists have been studying an eclipsing binary that has a record period of 69.1 years and a total eclipse which is 3.45 years long (1). The length of the eclipse may be a record too. The eclipse depth is from 10.8 magnitude to about 15. The last eclipse was from 2011 to 2015. The next one will, therefore, not start until 2080.

Below is an artist's impression of the system which was published in 'Nova' which is a publication of the American Astronomy Society (2).

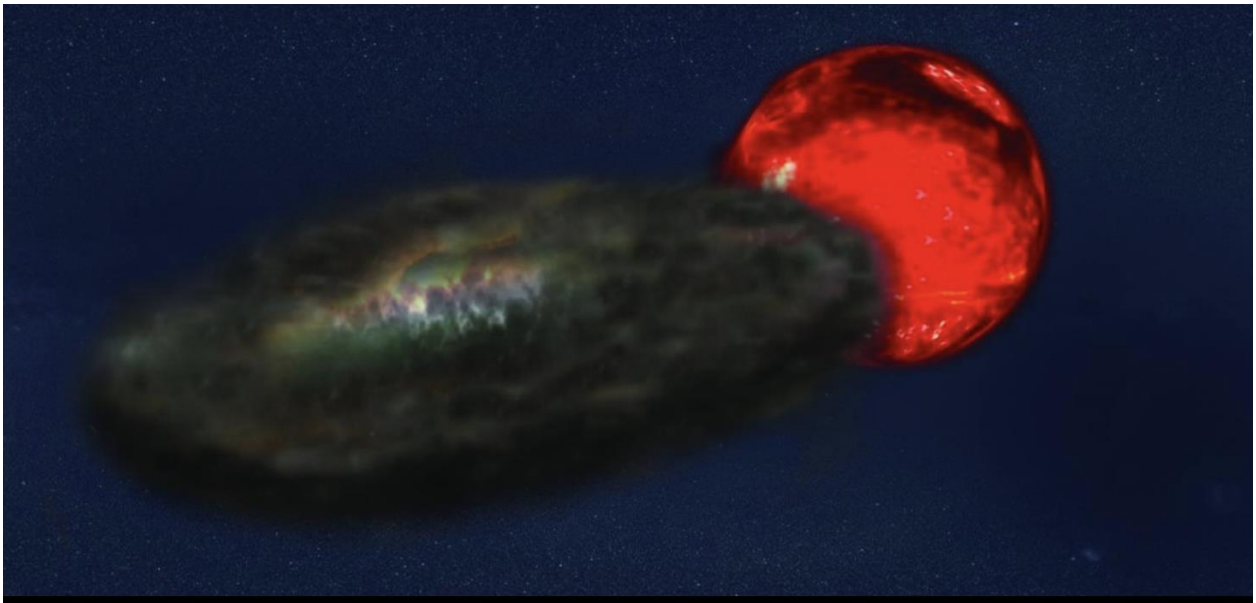

Artist's illustration of TYC-2505-672-1, a binary star system consisting of an M giant and a companion that is possibly shrouded by a circumstellar disk. [Vanderbilt University/Jeremy Teaford]

The system and the study are of interest because amateur astronomers contributed to the data that allowed the period to be determined.

The study explains the unusual length of the eclipse by suggesting that the eclipse is not just due to two stars. One of the stars is surrounded by a large disk. The system may be similar to the Epsilon Aurigae system. The authors of the paper suggest that the disk represents the stripped off atmosphere of a red giant. How this would occur and how a large opaque circumstellar disk would be created is not clear.

Eclipsing Binaries as distance indicators

A paper in *Nature* (3) describes the use of Eclipsing Binaries to determine the distance to the Large Magellanic Cloud (LMC) which is important in deriving the Hubble Constant. Using Eclipsing Binaries can apparently be more accurate than the previous method of using the very abundant LMC Cepheid population. The eclipsing binary method had previously applied to the LMC using bright early-type star systems, but this had proved to be less accurate than the Cepheid method.

With modern telescopes it is possible to analyse long period, late type, eclipsing binaries composed of cool giant stars. The paper records the study of eight of these systems. It was possible, using these systems, to make more accurate measurements of the distance to the LMC. Cepheid variables suggested a distance of 160,000 light years. The latest Eclipsing Binaries method suggests a distance of 163,000 light years.

This work has been made possible by the instrumentation at the La Silla Observatory in Chile. It is claimed by the ESO that their 3.6 metre telescope, now home to the High Accuracy Radial Velocity Planet Searcher (HARPS), is a spectrograph with unrivalled precision.

Because the LMC has geometry and depth the eight chosen systems were chosen as they were very close to the center of the LMC.

NASA's Fermi Detects First Gamma-Ray Eclipses From 'Spider' Star Systems

A 'Spider' Star system is a binary system where a star has a companion which is a pulsar. The pulsar is sufficiently near the star to erode material from its envelope by the pressure of the radiation that it emits.

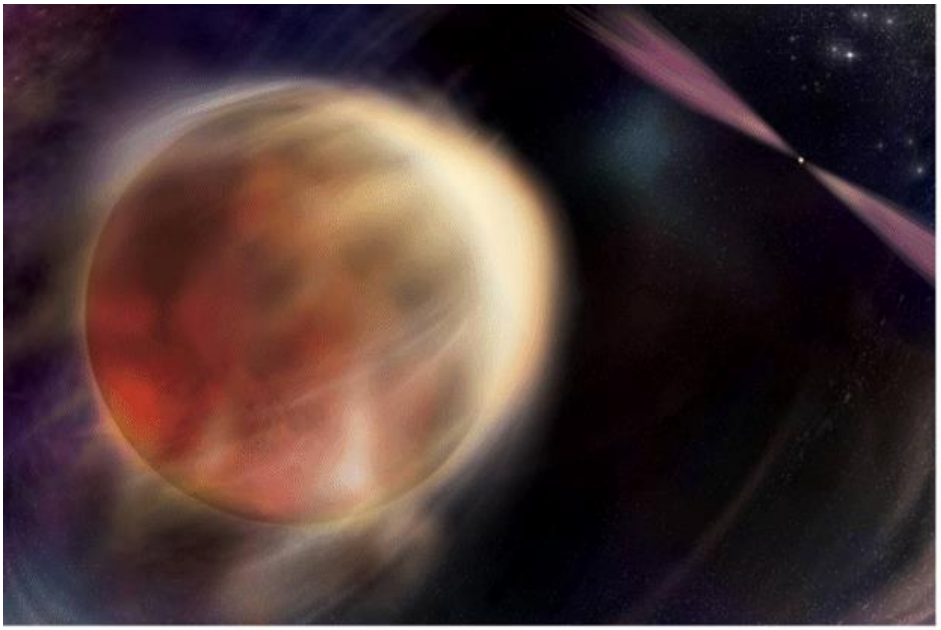

An orbiting star begins to eclipse its partner, a rapidly rotating, superdense stellar remnant called a pulsar, in this illustration. The pulsar emits multiwavelength beams of light that rotate in and out of view and produces outflows that heat the star's facing side, blowing away material and eroding its partner.
Credits: NASA/Sonoma State University, Aurore Simonnet

NASA 's Fermi Gamma Ray Telescope was launched into low earth orbit in 2008. It was initially considered to have a five-year life, but it continues operating to this day. It has been responsible for many discoveries. It studies gamma ray bursts. The Fermi instrument has been looking at 5 Spider systems which happen to be eclipsing binaries where the eclipsed light includes gamma rays. Above is an artist's impression of one of these systems.

The data resulting from Fermi can be used to estimate the mass of a pulsar (4). The study was published in January 2023 (5).

References

1: Joseph E. Rodriguez et al 2016 *AJ* **151** 123. doi:10.3847/0004-6256/151/5/123

2: https://aasnova.org/2016/05/02/record-breaking-eclipsing-binary/#

3: 'An eclipsing binary distance to the Large Magellanic Cloud accurate to 2 percent' Nature 495,76-79 (2013)

4: https://www.nasa.gov/feature/goddard/2023/nasa-s-fermi-detects-first-gamma-ray-eclipses-from-spider-star-systems

5: "Neutron star mass estimates from gamma-ray eclipses in spider millisecond pulsar binaries": Nature Astronomy 7. 45-462 (2023).

The open cluster star HD 281159 is revealed as an eccentric eclipsing binary and probable β Cephei variable.

John Greaves and
Christopher Lloyd

cl57@ymail.com

Examination of TESS photometry of the dominant star in the Open Cluster IC 348 shows it to be a 1.9340-day eccentric, e ~ 0.23, detached eclipsing binary that shows apsidal motion, but also has a multiperiodic pulsation signature, probably of a β Cep variable.

Introduction

HD 281159 (BD+31° 643) is a bright, *V* = 8.5, early-type star and is largely responsible for illuminating the adjacent reflection nebula, van den Bergh (vdB) 19. It is the brightest star within and lies at the heart of the young open cluster IC 348, which together with vdB 19 mark the north-eastern end of the Perseus Molecular Cloud and Perseus OB2 association complex, which itself is part of a much larger region of star formation incorporating the Taurus-Auriga Complex [1] referred to as the Perseus-Taurus Shell or Superbubble [2]. The vicinity of HD 281159 is shown in Figure 1 and the large variation in local structure is obvious, from the heavily obscured star forming region in the middle, to the very young dense cluster NGC 1333 at the bottom, with IC 348 at the top.

However, HD 281159 itself has long been known as a visual multiple system with the closest two components separated by 0.6 arc seconds discovered by Burnham in 1880, having *V* = 9.28 and 9.51 (see WDS 03446+3210, CCDM 03446+3210, ADS 2730). More distant and fainter components have also been found; Component C, also confusingly referred to as D, at 23 arcsec (SFT 439), and Component E at 44 arc seconds (WAL 24). The *Gaia* DR3 data for these stars are given in Table 1 and the parallaxes give a distance of 351 ± 9 pc for the central pair. The *Gaia*-derived distance of Bailer-Jones et al. [3] is consistent with this value. The other two components are placed at 279 and 312 pc, so would appear to be unconnected with the central pair. The mean distance to IC 348 has been measured recently at 311 ± 32 and 321 ± 10 pc [4, 5], but star formation occurs over some 290–350 pc [6], so HD 281159 would appear to be on the far edge of the cluster. At that distance the projected separation of components AB would be 210 AU, so they could be gravitationally bound, but in a cluster this happenstance proximity is no guarantee of a physical association. Having said that,

Table 1: *Gaia data for the visual companions*

		r	*RA*	*Dec*	*π*	*σ*	*G*	*BP*	*RP*	*BP-RP*
		“			mas	mas				
A		0.0	03 44 34.188	+32 09 46.13	2.853	0.075	8.888	8.715	7.637	1.078
B	BU 880	0.6	03 44 34.209	+32 09 46.62			9.136	8.722	7.645	1.076
AB							8.252			
C/D	STF 439	23.7	03 44 35.361	+32 10 04.59	3.581	0.162	9.871	10.456	9.096	1.359
E	WAL 24	43.9	03 44 30.815	+32 09 55.8	3.208	0.028	11.488	12.000	10.794	1.206

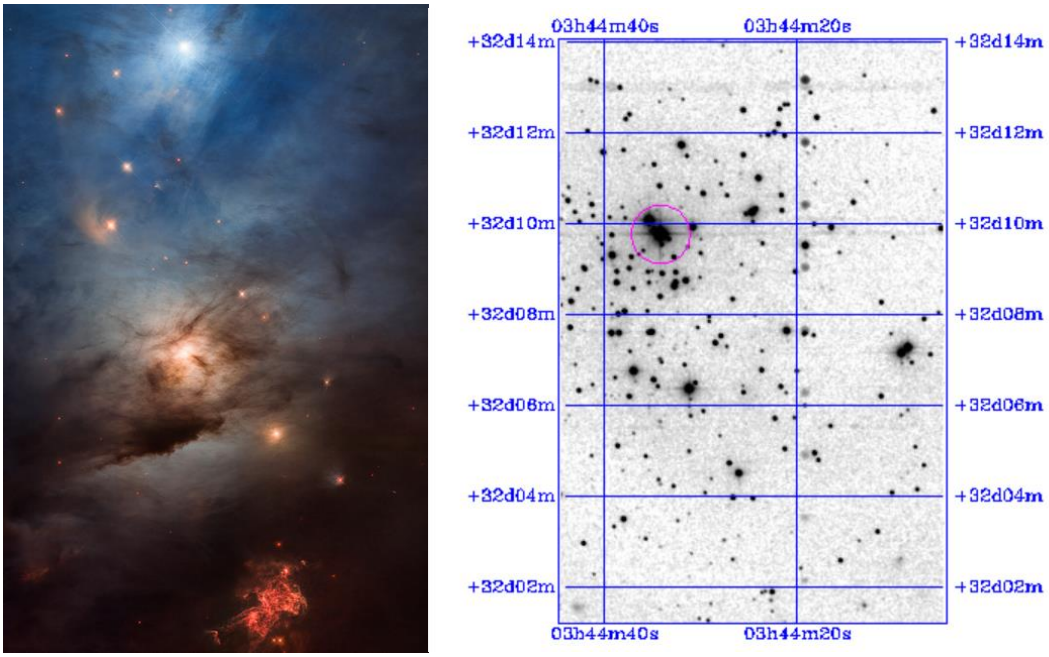

Figure 1: (Left) A composite Hubble image of part of the Perseus molecular cloud and Perseus OB2 association with HD 281159 dominating the reflection nebula vdB 19 at the top and NGC 1333 at the bottom. The picture is arranged at an artistic angle with north at about 45° towards the top right (Image courtesy of NASA/ESA/STScI). (Right) A J-band image at a similar scale, but different centre and orientation, from the Interactive 2MASS Image Service covering in a region of ~ 13×9 arc minutes around HD 281159 showing the stars of the IC 348 cluster that are partially obscured in the optical.

components AB and C are three of the brightest stars in the cluster so it is tempting to group them together. The *Gaia* photometry gives ΔG = 0.25 between components A and B, and the combined G = 8.252. Components C and E are $1^{m}.0$ and $2^{m}.6$ fainter than A respectively. The respective BP and RP magnitudes of A and B are suspiciously similar, which suggests issues with the processing. Also, Component B does not yet have an independent parallax, and although C is apparently discordant, the uncertainty on its parallax is disproportionately large, so there are likely to be revisions in later releases. The widely reported spectral type of the composite AB pair is B5V, but it is also listed as B3–4 [7]. However, the star has long been recognized as a velocity variable [8–11], so one component is an unrecognized spectroscopic binary. Components C and E are both listed as A2 [7].

TESS data

HD 281159 has been observed by the Transiting Exoplanet Survey Satellite (TESS) [12] during November 2019 in Sector 18 at the standard 30-minute cadence, from August to November 2021 in Sectors 42, 43 and 44 at the 10-minute cadence, and also during November 2022 in Sector 58 with a much higher cadence of 200 seconds. The data were extracted from the Full-Frame Images using the *Lightkurve* package [13] and restricted to HARD quality in *Lightkurve* parlance. The fluxes were measured using a slightly restricted version of the default aperture created within the routine, so as to produce a more regular outline. Although the star is bright, the high background during parts of the orbit did limit the data. The resulting light-curve is relatively smooth but some discordant sections were removed and additional flattening with a wide filter was required to correct variation in level through the TESS orbit, as is often the case. The TESS pixel size is nominally 21 arc seconds so components A and B are irrevocably blended, and the FWHM of the PSF is 40 arc seconds, so Component C is also within the profile, but it is a magnitude fainter. The other nearby stars are too

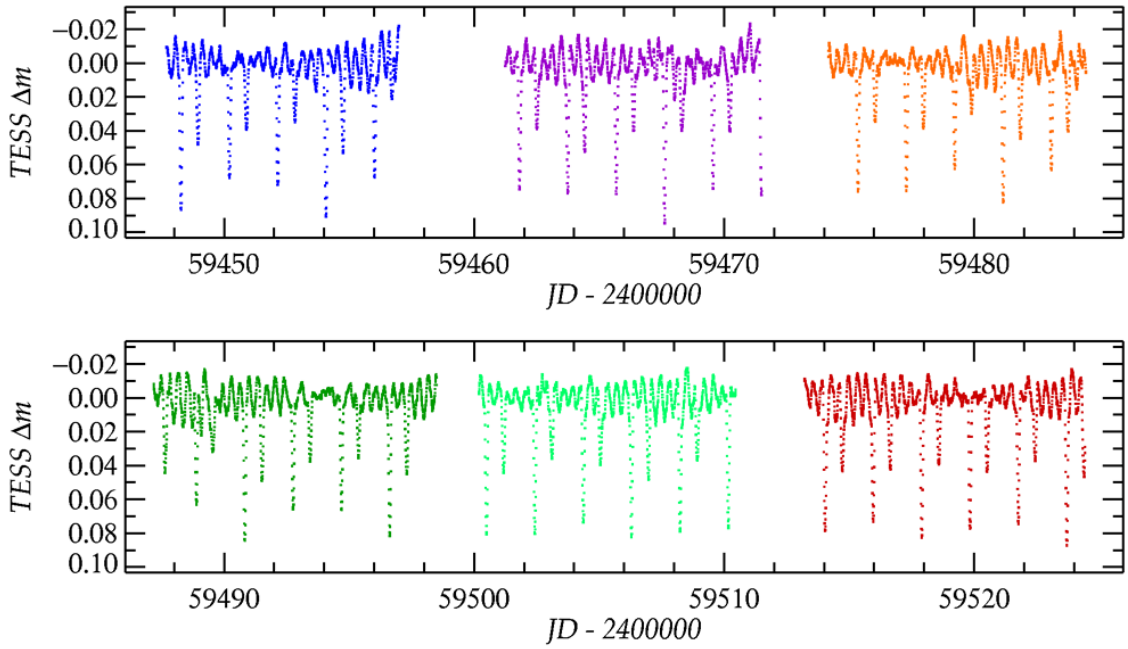

Figure 2: Epoch plot of the TESS data from Sectors 42, 43 and 44, with the different half-sectors shown in different colours. The individual eclipses are clearly seen and the influence of the β Cep variation is obvious. Even at this stage the displacement of the secondary eclipse from phase 0.5 is obvious.

faint to contaminate the photometry, and Component E at 44 arc seconds and $2^{m}.6$ fainter is unlikely to have an influence.

The TESS sectors naturally divide into two due to the 1–2 day break for the data downlink so the light-curve comprises ten sections of $\sim$11 days of mostly continuous data. The normalized fluxes are converted to magnitudes and are shown for Sectors 42, 43 and 44 in Figure 2. Visual inspection of the light-curve immediately shows that the star is an eclipsing binary with a period near two days and there is also a coherent, high-frequency variation with an amplitude of $\sim 0^{m}.01$ affecting both the out-of-eclipse level and the depths of the eclipses. The primary eclipse has a depth of $\sim 0^{m}.07$ and the secondary $\sim 0^{m}.04$. The secondary eclipse is also very obviously displaced from phase 0.5.

The low-amplitude variation

The period of the eclipsing binary was initially determined from the high-order Fourier fit to all the data at close to $1^{d}.934025$, and the measurements around the eclipses were removed to leave the out-of-eclipse values, under the assumption that this region of the light-curve was probably flat. These measurements were then subjected to a period analysis through repeated application of an iterative period-search, fitting and prewhitening loop. Frequencies were identified through a Discrete Fourier Transform (DFT) periodogram, and then refined and removed using a multifrequency Fourier fitting routine of the form

$$V_k = \sum_{j=1}^{m} a_j \cos\left(2\pi f_j T_k + \varphi_j\right) + c_z \qquad (1)$$

where V_k is the observed magnitude at time T_k, $j = 1,\ldots,m$ is the number of frequencies, and there is just the single harmonic for each frequency, φ_j is the phase offset for each frequency j, and c_z is the constant level for any particular subset (half sector) of the data. The data were analysed for the three epochs based on continuity. Sector 18 has the lowest cadence and consequently has the largest uncertainties. Sectors 42, 43 and 44 were treated together as they provide a substantial continuous

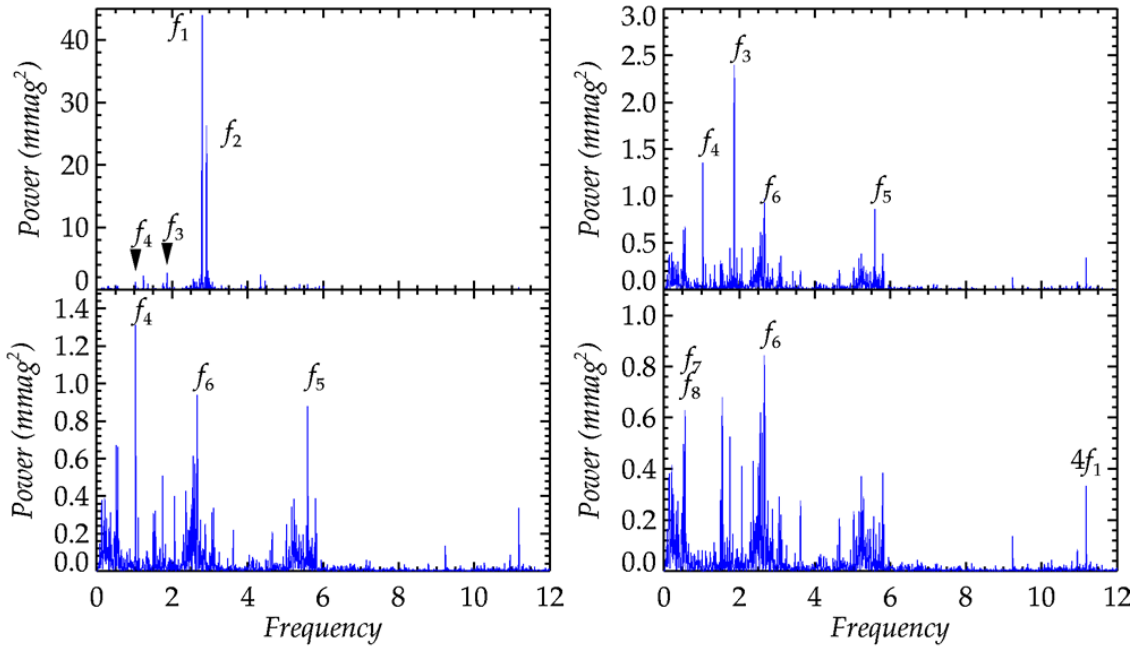

Figure 3: DFT periodograms of the TESS data from Sectors 42, 43 and 44 prior to the removal of any frequencies (top left) showing the two dominant frequencies, and the barely visible f_3 and f_4. The next two panels show the DFT after the removal of f_1 and f_2 (top right) and f_3 (bottom left). The final panel (bottom right) shows the DFT after the removal of f_4 and f_5. The two frequencies f_7, and f_8, which is the orbital frequency, are unresolved at this scale, and the last feature of interest is $4f_1$. The noise level at higher frequencies is less than that seen in this range and is generally < 0.01 mmag^2 with a few occasional features up to ~0.05 mmag^2.

run at a better cadence and these are the results that will be discussed in more detail. Sector 58 has by far the highest cadence but it lacks resolution provided by a longer baseline.

The results show that the star - one of the stars - is a multi-periodic variable with two overwhelmingly dominant frequencies, and a number of other significant frequencies. Many of the same frequencies appear in the results for all three sets but Sector 18 is clearly noisier and some of the features are not replicated in the other sets. The most significant results for all three epochs are listed in Table 2 and DFTs of different stages of the extraction process for Sectors 42, 43 and 44 are shown in Figure 3.

Table 2: ***Significant frequencies for the three epochs***

id	*f*	*amp*	*f*	*amp*	*f*	*amp*
		mmag		*mmag*		*mmag*
f_1	2.79601(59)	5.95(17)	2.796096(55)	6.55(5)	2.79601(14)	6.10(5)
f_2	2.91429(94)	3.43(20)	2.912053(75)	4.84(5)	2.91228(17)	5.07(5)
$f_3 \sim 2f_1/3$	1.8700(25)	1 36(19)	1.86639(23)	158(5)	1.86439(62)	1.38(5)
$f_4 \sim 2f_{orb}$			1.03395(38)	1.01(5)		
$f_5 = 2f_1$			5.59211(37)	0.94(5)		
f_6			2.66067(38)	0.93(5)		
f_7			0.56215(43)	0.91(5)		
$f_8 = f_{orb}$			0.51879(47)	0.86(5)		
$f_9 = f_2 - f_1$					0.13115(69)	1.29(5)
f_{10}	0.5061(26)	1.29(20)			0.50530(65)	1.35(6)
$4f_1$			11.184	0.065		

The two dominant frequencies are f_1 = 2.79610 and f_2 = 2.91205 cycles.d^{-1} with amplitudes of 6.6 and 4.8 mmag respectively. Most of the other significant frequencies are harmonics of f_1, and there is one major combination frequency, $f_2 - f_1$, and other components are related to the eclipsing binary period, f_{orb}. It is possible that the eclipsing binary variation has not been fully removed as the out-of-eclipse region has simply been assumed to be flat, so at this stage it is not clear if the orbital period has been detected directly in the short-period variations or is an artefact of simple processing. The low amplitude and dominant frequencies suggest that the short-period variable is either a Slowly Pulsating B star (SPB), a *γ* Doradus, *β* Cephei or *δ* Scuti star. Both the SPB stars and *γ* Dor variables have dominant frequencies around 1 cycles.d^{-1}, and a recent large study using *Gaia* data shows that the distribution falls off rapidly with only a small percentage of stars reaching f_1 [14, 15]. The opposite is true of the *δ* Sct stars which have dominant frequencies in the $f \sim 10$–30 cycles.d^{-1} range, although many do show lower frequency variations as well [16]. The *β* Cep stars have dominant frequencies over a broad peak in the $f \sim 4$–8 cycles.d^{-1} range [17], so in terms of the dominant frequency HD 281159 is most consistent with the *β* Cep stars. The other reason for preferring this classification over the *γ* Dor relates to the amplitude of the pulsation. *β* Cep stars are more luminous typically, O9–B5, as opposed to late-A to early-F, so are ~2 magnitudes brighter than *γ* Dor stars. The typical pulsation amplitude of both groups is ~5 mmag but being much less luminous any *γ* Dor variable would be significantly more diluted by the other components of the system. The variation as observed is typical of *β* Cep stars so it probably originates in the most luminous star. The combined spectral type of the AB system is generally accepted as B5V, and although this is towards the cool end of the *β* Cep range, one star must be earlier than this. One of the components A, B or C must be the eclipsing binary with the attendant drop in luminosity of the individual stars. If Component A is the binary, then it is possible for the primary to be a *β* Cep star and still produce the observed difference in eclipse depths. The same is probably not true for B, although it is only slightly fainter than A, and certainly not for C, which is a magnitude fainter. The most likely conclusion is that Component A is the binary and the source of the *β* Cep variation, and similar systems are known [18].

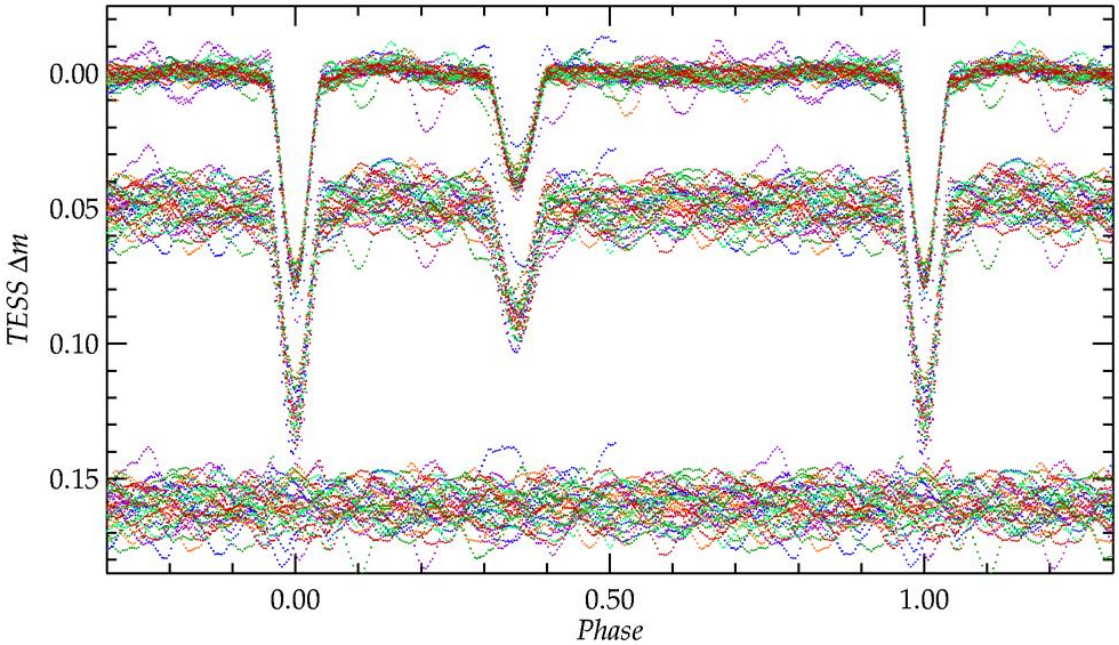

Figure 4: Phase diagram of the TESS data from Sectors 42, 43 and 44 folded on the best period, showing the data corrected for the *β* Cep variations (upper), the original data offset by $0^m.05$ (middle), and (bottom) the residuals of the original data from their Fourier fit offset by $0^m.16$. The residuals, inside and outside eclipse, show no obvious difference so both are affected by the short-period variation. The huge displacement of the secondary eclipse is obvious. There is some indication of a possible reflection effect in the out-of-eclipse section near phase 0.2, and a possible low-amplitude wave in the other section. The discordant runs in the corrected data can mostly be traced to poorly normalized data at the ends of the half-sectors. The different half-sectors are shown in different colours.

The eclipsing binary variation

In an effort to produce a more reliable light-curve of the eclipsing binary, the short-period variation, as calculated for each of the three epochs as described above, has been removed from the whole data set, including the eclipses. The phase diagram of Sectors 42, 43 and 44 is given in Figure 4 and shows the original and pulsation-corrected data. The period is again determined by a high-order Fourier fit and this allows the optimum phasing of the two minima to be measured, which in this case gives $\varphi_2 = 0.352$, for this epoch. The displacement from the circular orbit position $\varphi_2 = 0.5$ indicates that the orbit is eccentric and using the first-order approximation that $e\cos\omega = \pi(\varphi_2 - 0.5)/2$ leads to $e\cos\omega \approx -0.23$, so places ω in the 180° quadrant and suggests a maximum eccentricity of $e = 0.23$. For an early-type star with a period less than 2 days that eccentricity is extreme and ranks amongst the highest known [19]. Some other simple observations can also be made from the light-curve. There is no obvious difference in the widths of the two eclipses, so given that the system is eccentric, most likely ω is close to 180°. The residuals from the fit to the original data show no significant variation with phase, and in particular inside and outside the eclipses, so it seems that the whole light-curve is similarly affected by the short-period variations. In theory this could exclude the primary as the source of the pulsations, however, the primary eclipse is so shallow that only $\sim$20% of the star is obscured, depending on the dilution, so unfortunately it provides little constraint. The eclipses are shallow, and even though there will be some dilution, they are still very partial, so the inclination of the system is probably low. The difference in the eclipse depths also suggests that the secondary component has perhaps half the luminosity the primary, through a combination of a smaller radius and lower temperature, again assuming $\omega \sim 180°$. There is some indication of a possible reflection effect in the out-of-eclipse section near phase 0.2, and it is possible that this could be responsible for the appearance of f_{orb} in the short-period variations. These is also a possible low-amplitude wave in the other section of the out-of-eclipse data.

The times of minima have been measured for all the individual half-sectors using a high-order Fourier fit and these are shown in the displacement plot, and O–C diagram in Figure 6. The displacement is simply the difference between the observed time of the secondary eclipse and its expected time at $\varphi_2 = 0.5$, as given by $D = t_s - t_p - P/2$ (see e.g., Guinan & Maloney [20]). It is immediately obvious that

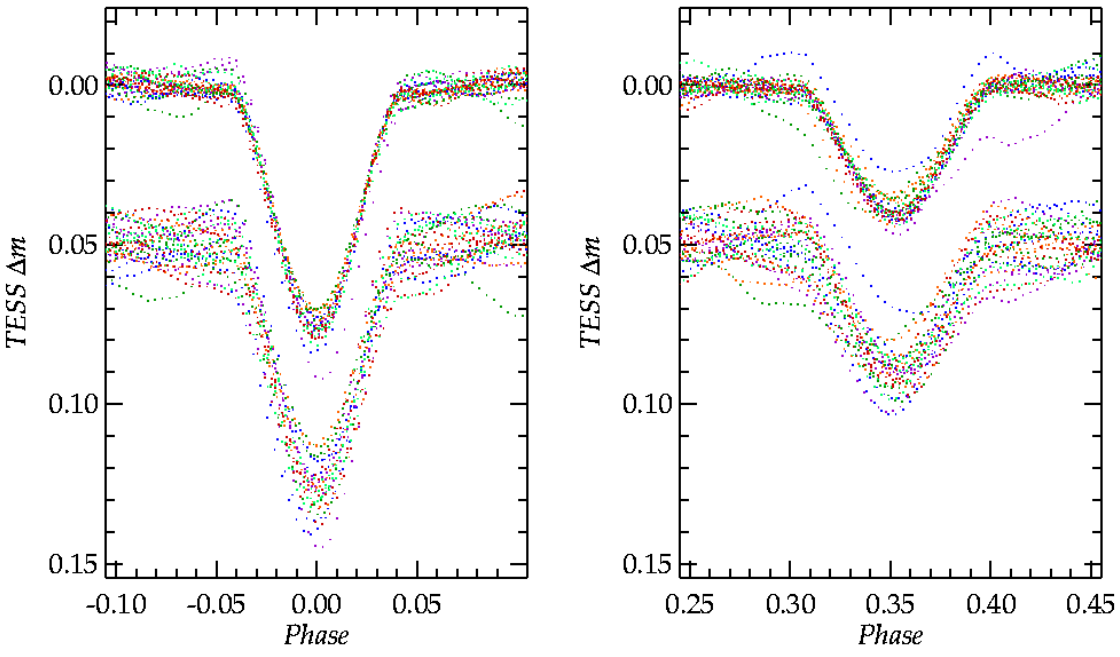

Figure 5: Detail of the primary and secondary eclipses.

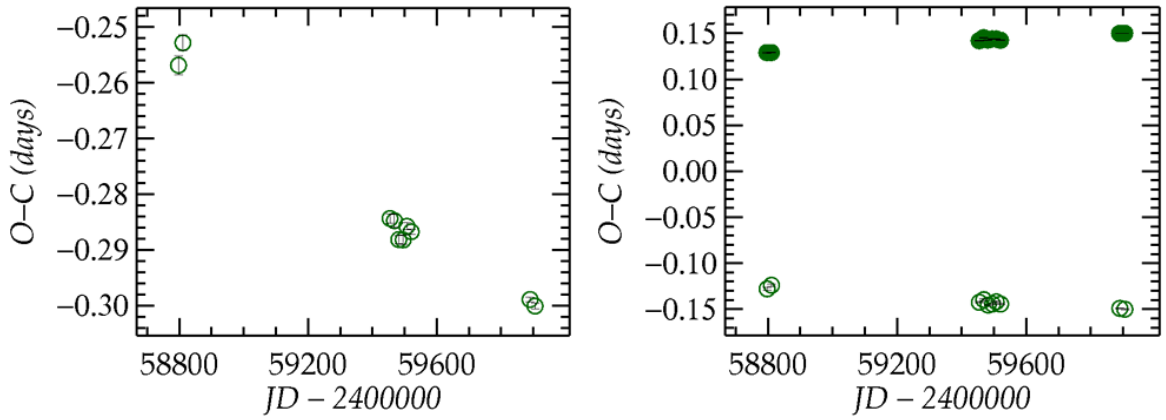

Figure 6: The Displacement and O–C diagrams of all the TESS data using the mean times of minima from each half-sector, with the primary minima shown as filled circles. The uncertainties are typically smaller than the symbols. (Left) The diagram shows the displacement of the secondary eclipse from $\varphi_2 = 0.5$ as described in the text. The displacement is still increasing but there is some indication that the rate is slowing. The changing displacement demonstrates a significant apsidal motion, which must have a short period. (Right) A first attempt at an apsidal O–C diagram using the mean ephemeris from Equations 2 and 3. The increasing separation of the minima can still be seen, but it is not as clear on this scale.

displacement of the secondary minimum changes with time, so not only is the orbit eccentric, but it also shows the clear indication of apsidal motion. There are insufficient epochs to reliably solve for e and $\dot{\omega}$, but some simple modelling suggests that the apsidal period, U, may be as short as 30–35 yr, and that the displacement may reach its maximum within 5 years. The implication of this is that there is probably a third body in the eclipsing binary system that is driving the apsidal motion. The weighted linear fits to the times of minima are for the primary minima alone.

$$BJD_{\mathrm{MinI}} = 2458796.50704(25) + 1.93403545(56) \times E \qquad (2)$$

and for just the secondary minima

$$BJD_{\mathrm{MinII}} = 2458796.24755(69) + 1.9339636(15) \times E \qquad (3)$$

but these will both evolve slowly with time.

Summary

HD 281165 is shown to be a complex system comprising the visual components AB at 0.6” and C at 24” that are included in the TESS aperture. Analysis of the TESS data from three epochs reveals that the system contain a $1^{\mathrm{d}}.9340$ detached eclipsing binary with eclipse depths of $0^{\mathrm{m}}.07$ and $0^{\mathrm{m}}.04$ and a low-amplitude multiperiodic variable with two dominant frequencies of $f_1 = 2.79610$ and $f_2 = 2.91205$ cycles.d^{-1} and amplitudes of 6.6 and 4.8 mmag respectively. The frequencies and amplitudes are most consistent with a β Cep variable that is luminous and less subject to the dilution of the other components. It is most likely that Component A is the binary and the source of the pulsations. The eclipsing binary orbit is elliptical $e \sim 0.23$, which is extreme for an early-type system, and further, there is clearly apsidal motion, probably with a short period, which indicates a third body in the eclipsing system. Further work is needed to improve the extraction of the TESS data and modelling of the eclipsing binary light-curve. With care and suitable equipment, it should also be possible to monitor the evolution of the eclipse timings from the ground.

Acknowledgements

The authors are pleased to acknowledge the use of the NASA/ADS, the SIMBAD database and the VizieR catalogue access tool. The authors acknowledge use of the USNO Washington Double Star Catalogue. This paper includes data collected by the TESS mission, which are publicly available from the Mikulski Archive for Space Telescopes (MAST). Funding for the TESS mission is provided by NASA's Science Mission directorate.

References

1. D. M. Krolikowski, A. L. Kraus, A. C. Rizzuto, *AJ*, **162**, 110 (2021)
2. S. Bialy, et al., *ApJ Lett*, **919**, L5 (2021)
3. C. A. L. Bailer-Jones, et al., *AJ*, **161**, 147 (2021)
4. M. Boyce, D. Ruiz-Rodriguez, J. H. Kastner, in *American Astronomical Society Meeting Abstracts #233* (2019), *American Astronomical Society Meeting Abstracts*, vol. 233, p. 266.03
5. G. N. Ortiz-León, et al., *ApJ*, **865**, 73 (2018)
6. C. Zucker, et al., *ApJ*, **869**, 83 (2018)
7. K. L. Luhman, T. L. Esplin, N. P. Loutrel, *ApJ*, **827**, 52 (2016)
8. H. A. Abt, E. S. Biggs, *VizieR Online Data Catalog*, III/4 (2015)
9. K. C. Steenbrugge, et al., *A&A*, **402**, 587 (2003)
10. M. Cottaar, et al., *ApJ*, **807**, 27 (2015)
11. H. Jönsson, et al., *AJ*, **160**, 120 (2020)
12. G. R. Ricker, et al., *Journal of Astronomical Telescopes, Instruments, and Systems*, **1**, 014003 (2015)
13. Lightkurve Collaboration, et al., 'Lightkurve: Kepler and TESS time series analysis in Python', Astrophysics Source Code Library, record ascl:1812.013 (2018)
14. C. Aerts, G. Molenberghs, J. De Ridder, *A&A*, **672**, A183 (2023)
15. L. A. Balona, et al., *MNRAS*, **415**, 3531 (2011)
16. J. A. Guzik, *Frontiers in Astronomy and Space Sciences*, **8**, 55 (2021)
17. J. Labadie-Bartz, et al., *AJ*, **160**, 32 (2020)
18. J. Southworth, et al., *MNRAS*, **497**, L19 (2020)
19. P. Zasche, Z. Henzl, M. Mašek, *A&A*, **652**, A81 (2021)
20. E. F. Guinan, F. P. Maloney, *AJ*, **90**, 1519 (1985)

Light curves and phase diagrams of more Eclipsing Binaries; two long period and two short period systems.

David Conner

david@somerbyconners.plus.com

Observations of four eclipsing binaries, including results for CD And which appear inconsistent with observations made by others.

AZ Cas

Light curve and phase diagram of the EA/GS+LC type eclipsing binary AZ Cassiopeiae / AZ Cas, from photometry of 313 images taken with the Open University COAST telescope between 2017 September 22 and 2023 March 25. All images were taken with a V filter.

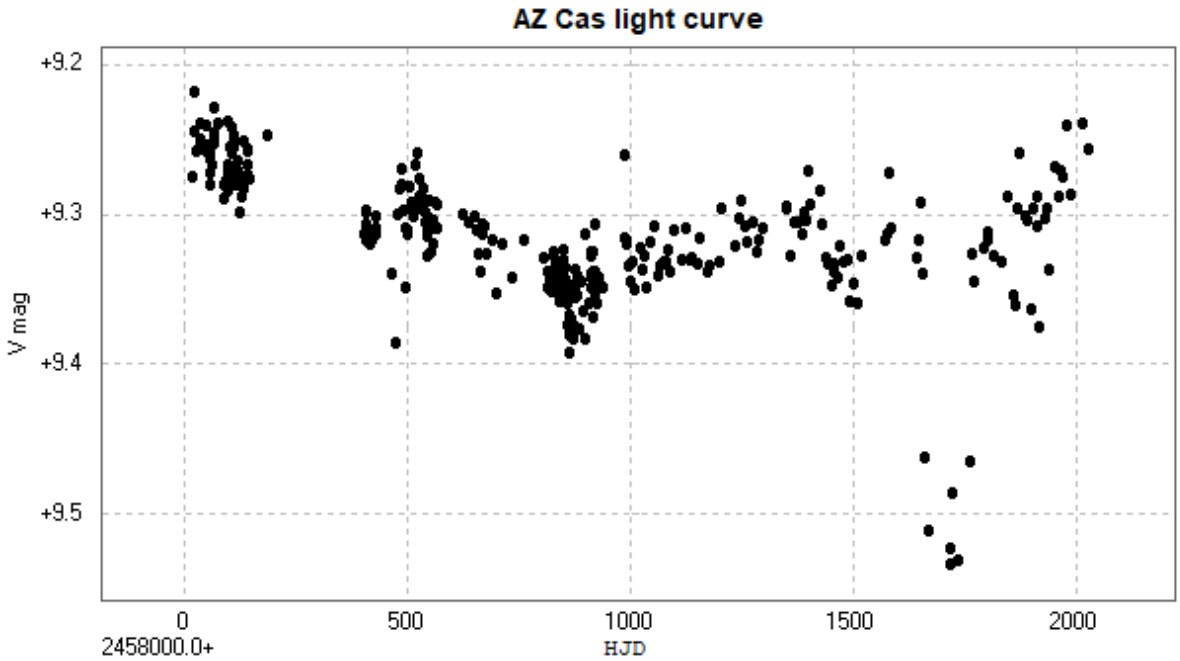

This star has catalogued periods of 3403.6 days (GCVS) and 3403.85 days (AAVSO VSX) [accessed 2023 May 15].

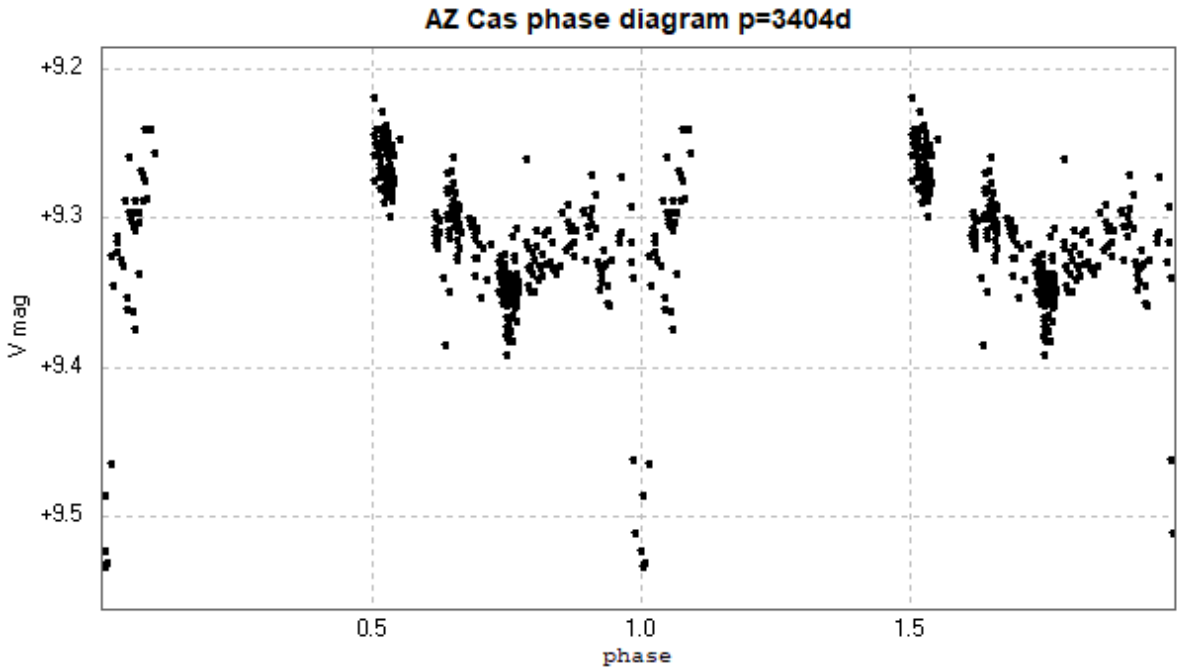

An enlargement at phase 0 (= phase 1.0) is below.

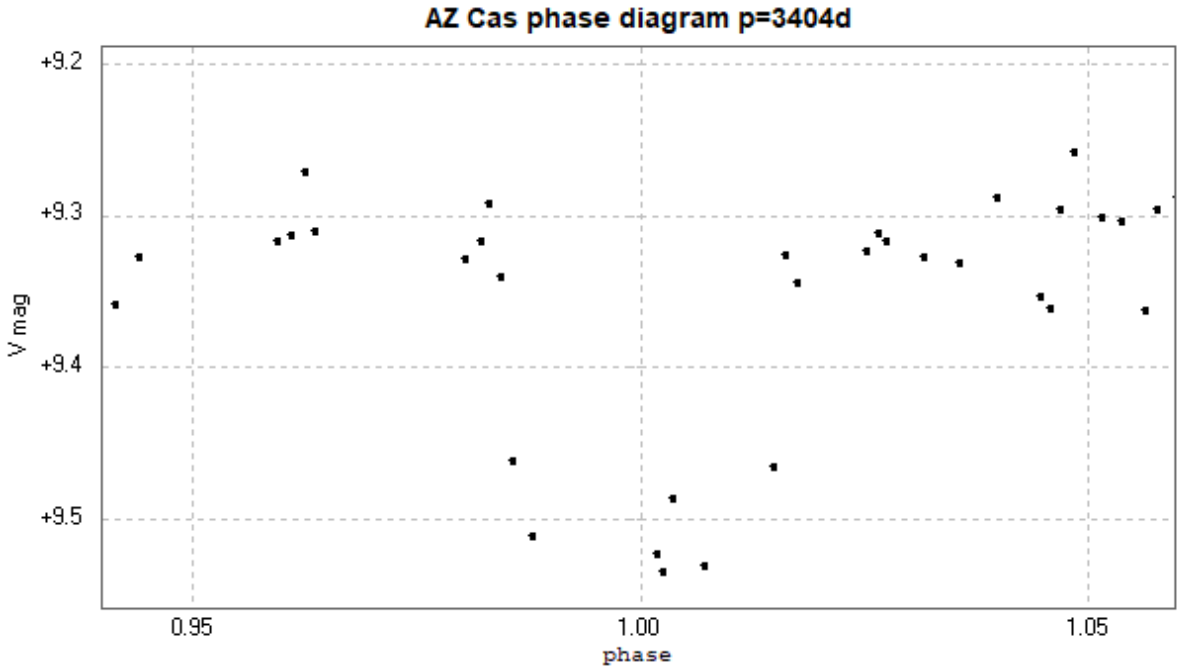

The 'dip' at approximately phase 0.76 is probably not an eclipse (the system has a highly eccentric orbit with e=0.55 *Cowley 1977*), but is more likely to be the result of variability of the red supergiant component (see type LC ref GCVS) . This is a complex system (see *Cowley et al 1977* and *Tempesti 1979*) and does typically show variation between primary minima. Its spectrum is given by the GCVS as M0eIb+B0-B1V and by the AAVSO VSX as F8-M0elb+B0/B1V [accessed 2023 May 14].

CD And

Light curves and phase diagrams of the EA type eclipsing binary CD Andromedae / CD And. These were constructed from 384 images taken between 2017 July 6 and 2023 March 18 with the Open University COAST telescope using a V filter.

74 observations had previously been obtained with COAST's precursor, The Bradford Robotic Telescope Cluster Camera (BRT), between 2013 September 30 and 2016 October 1. Although different comparisons were used (due to different fields of view) and different filters were used ('green' instead of V), they were included in the light curve below. The BRT results are in red and the COAST results are in black.

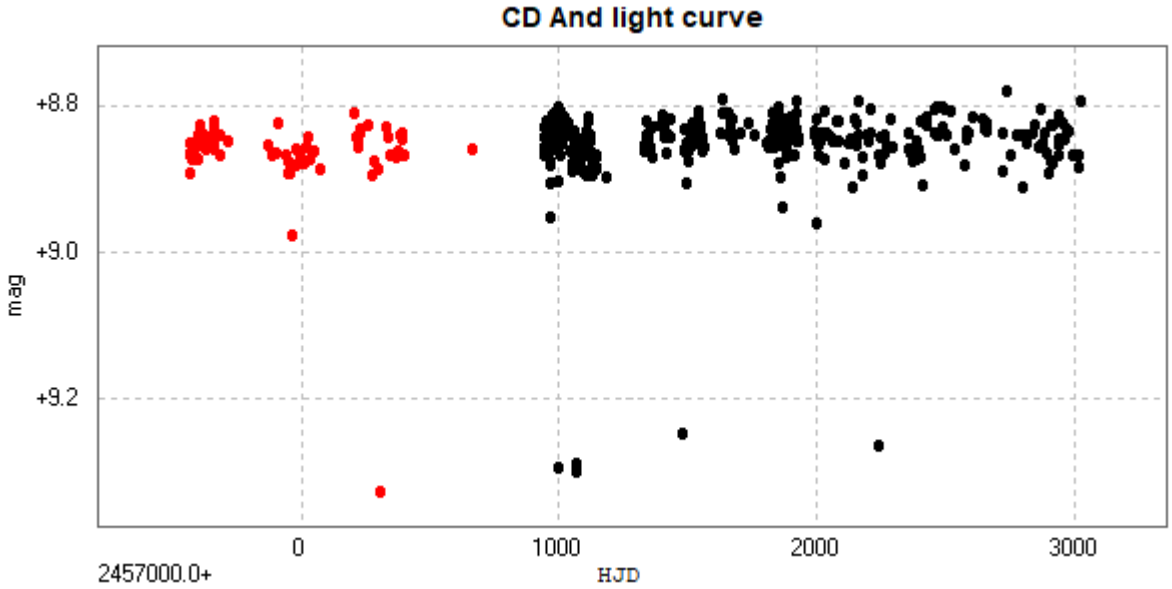

The catalogue value for the period of this star is 68.8832 days (GCVS, AAVSO VSX, Kreiner) [accessed 2023 May 14]. This period generated the following phase diagram.

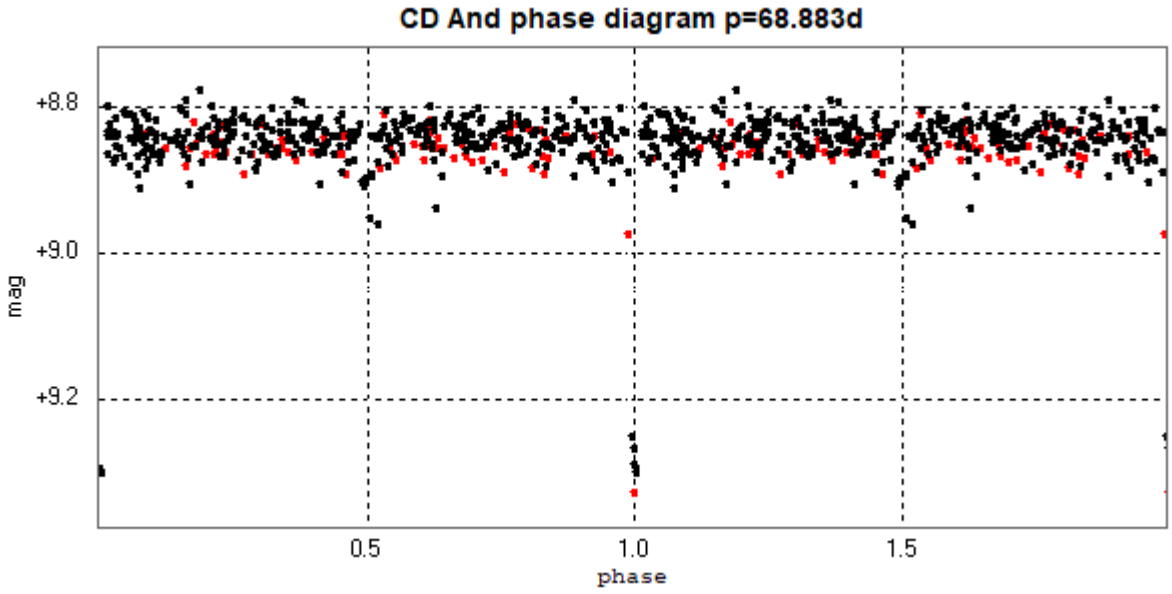

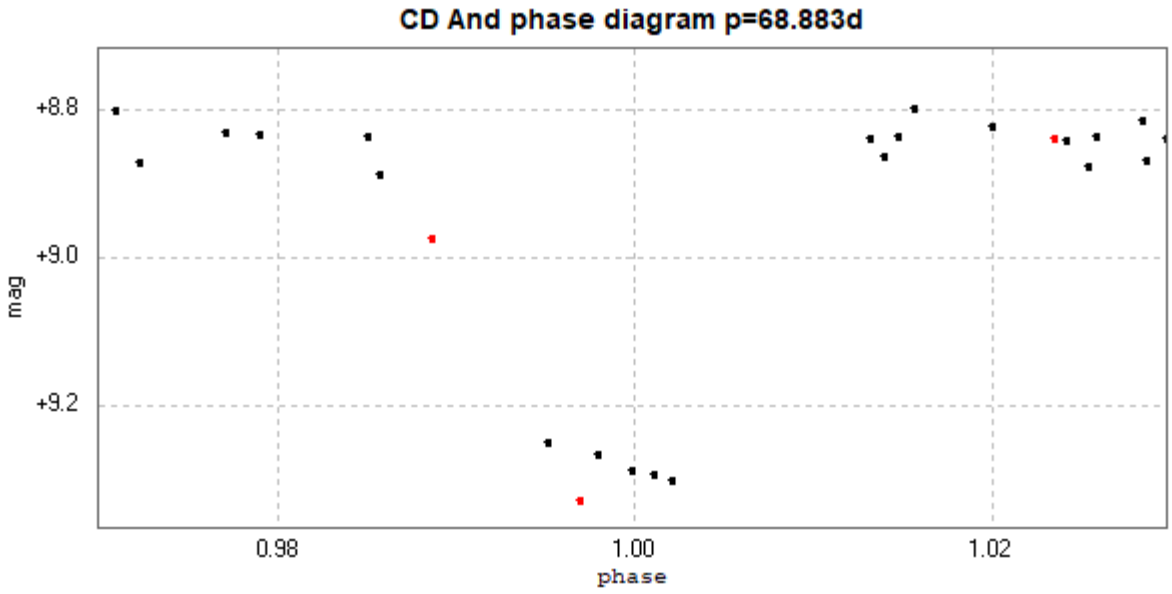

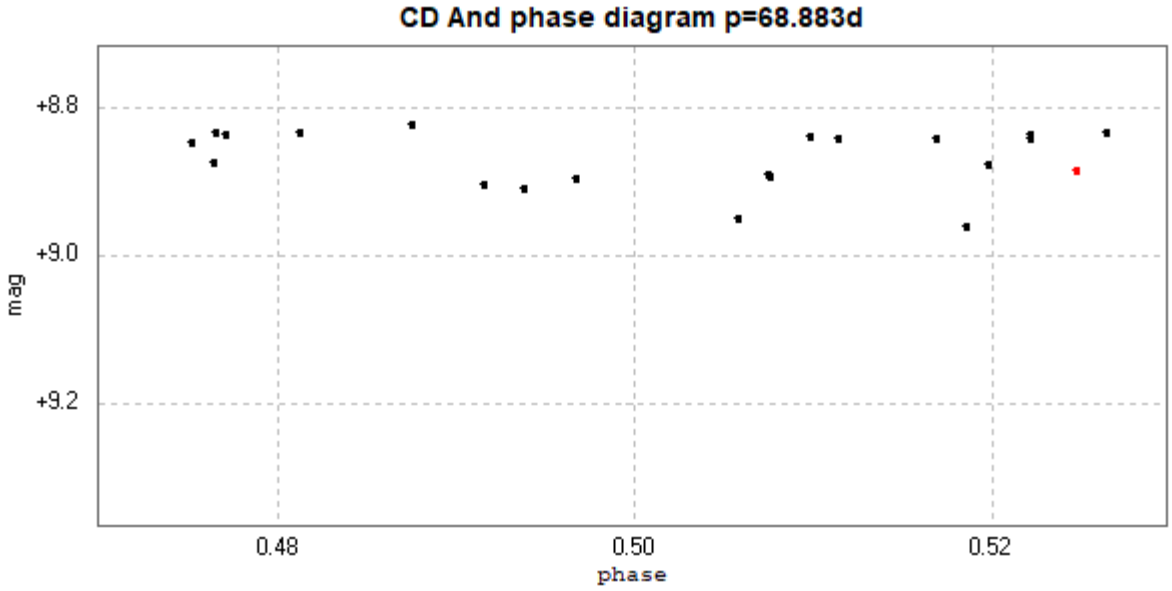

According to the GCVS, the primary and secondary minima should both have a depth of 0.5 mag. From these observations there is indeed a primary minimum of approximately 0.5 mag depth, but a secondary minimum is not conspicuous in this data. However, doubling the period to 137.77d resulted in the following phase diagram.

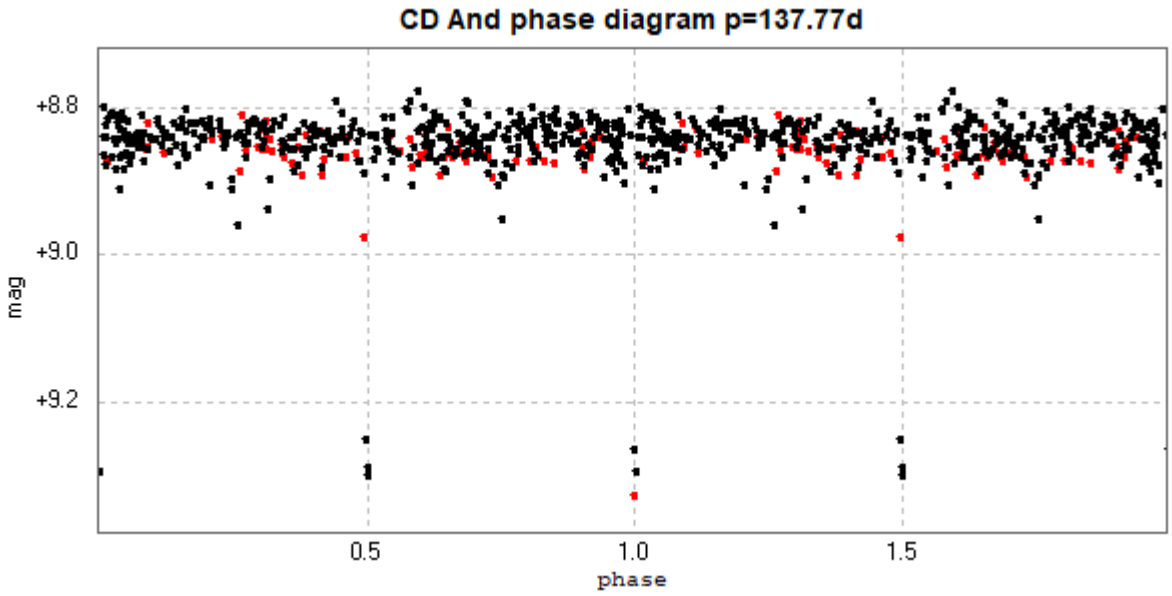
CD And phase diagram p=137.77d
+8.8
+9.0
+9.2
mag
0.5
1.0
1.5
phase

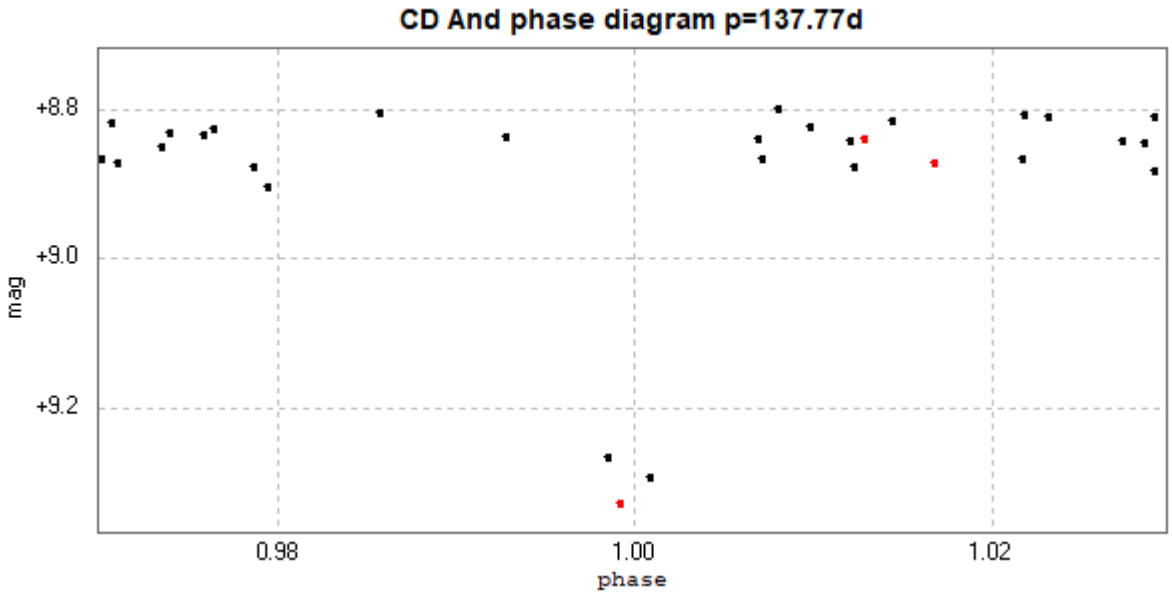
CD And phase diagram p=137.77d
+8.8
+9.0
+9.2
mag
0.98
1.00
1.02
phase

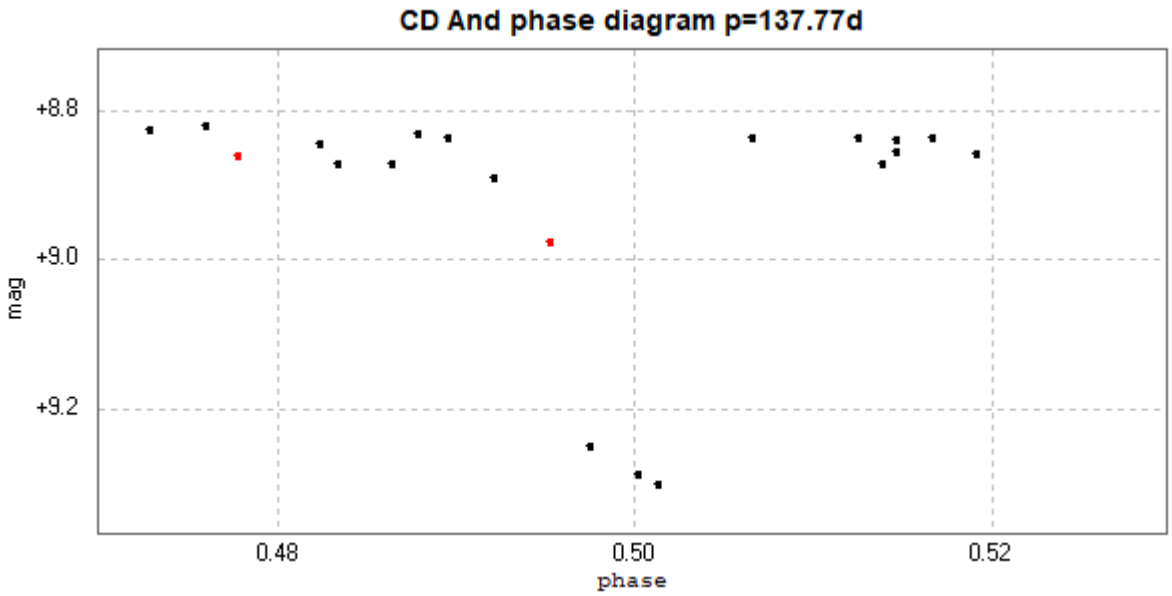
CD And phase diagram p=137.77d
+8.8
+9.0
+9.2
mag
0.48
0.50
0.52
phase

Here, the depths of the primary and secondary minima are consistent with the GCVS data, and their widths are superficially consistent with each other. However, this period is *inconsistent* with radial velocity data obtained by Imbert, M (2002) which does indeed indicate that the 68.8832d period is the correct one.

This system needs more observations to investigate this apparent discrepancy regarding the secondary minimum and it remains in my observing program.

Z Per

Following up to my article published in circular 192 (2022 June), a light curve and phase diagram of the EA/SD eclipsing binary Z Persei / Z Per. These were constructed from photometry of 83 images taken with the Open University COAST telescope, between 2019 June 15 and 2023 April 2, using a V filter.

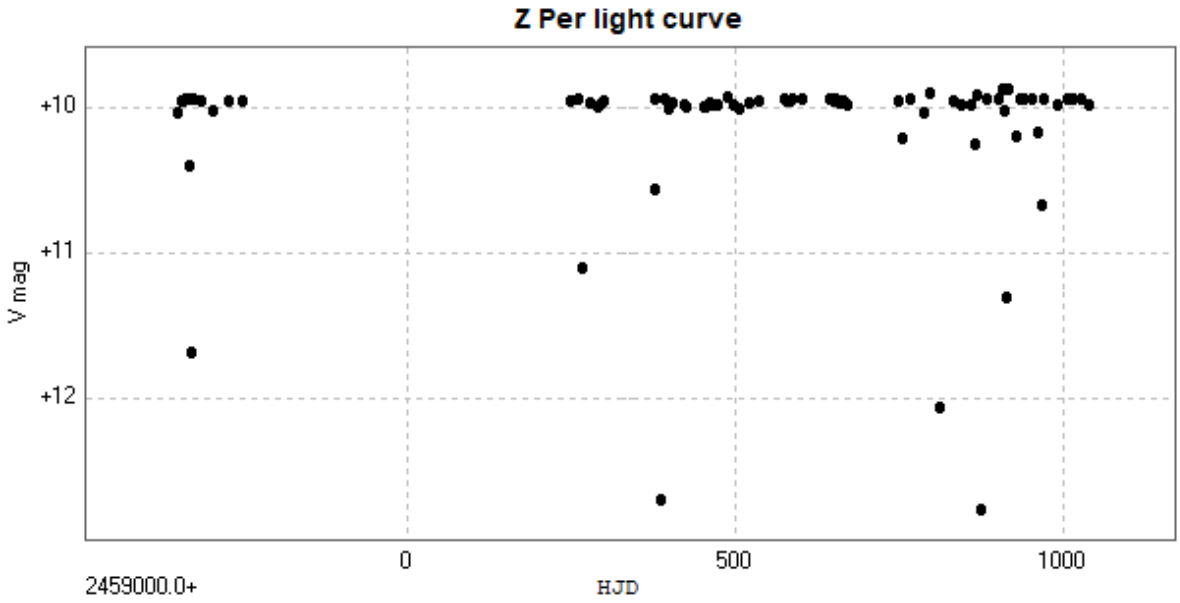

The catalogue periods for this star are variously given as 3.0563066d (GCVS) and 3.0562360d (AAVSO VSX) [accessed 2023 May 11].

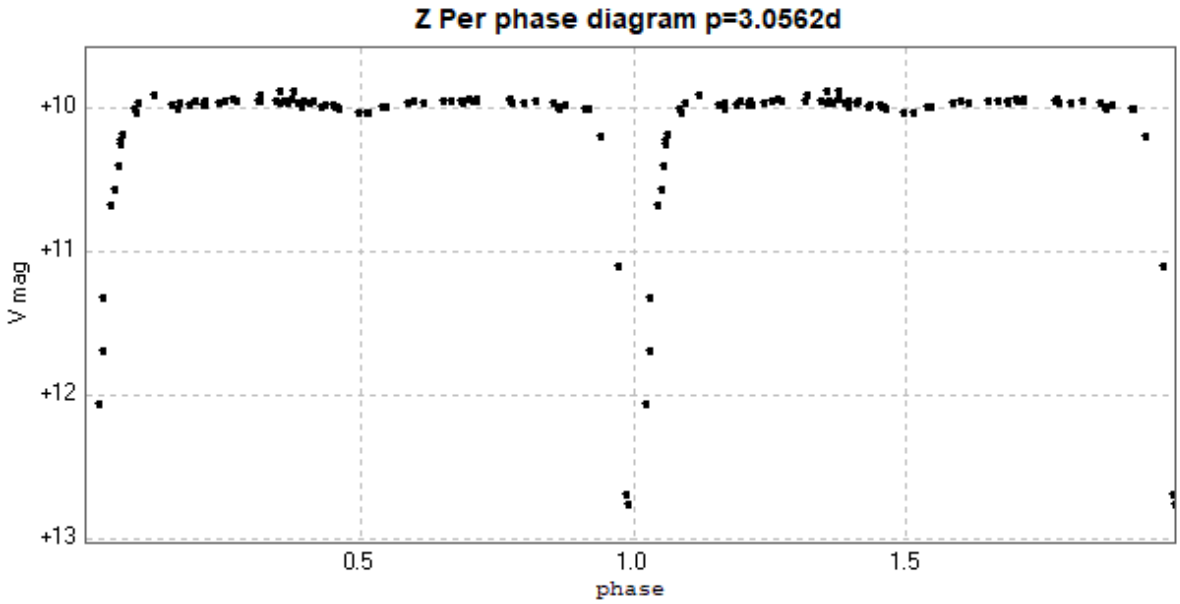

(Given the frequent poor weather at the site and technical issues affecting the COAST system I have now dropped this variable from my observing program in order to concentrate on long period eclipsing binaries.)

IM Aur

Light curve of a primary minimum of the EA type eclipsing binary IM Aurigae IM Aur obtained on 2022 December 14. This was constructed from photometry of unfiltered images taken with the '2 inch Titan' at my private observatory near Melton Mowbray, Leicestershire.

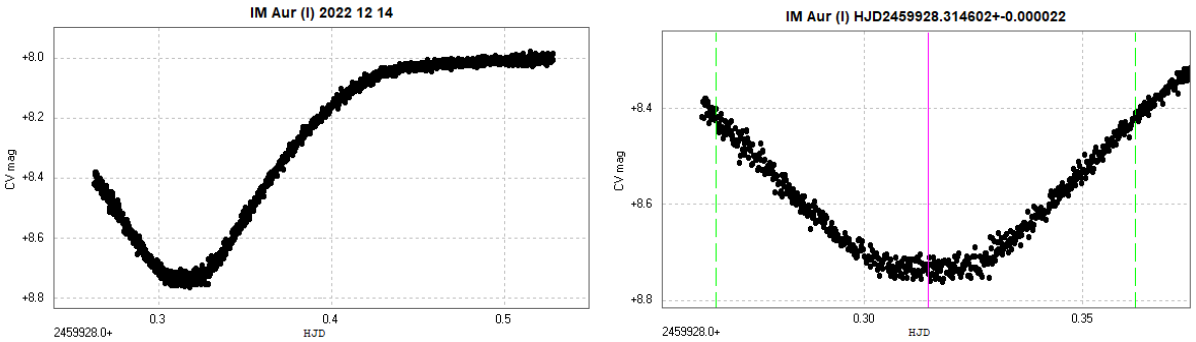

The time of minimum was obtained by Peranso.

The catalogued period for this system is given as 1.2472863d (GCVS, Kreiner) and 1.24728553d (AAVSO VSX) [accessed 2023 May 14]. There is significant o-c activity with this system (Kreiner). The following articles discuss this system in some detail; Bruhweiler et al (1986) and Borkovits et al (2002).

Time of minimum

Star	HJD of min	Filter	Error	Type of minimum
IM Aur	2459928.31460	CV	0.00002	Primary

More information can be found on my website.

Recent minima of various Eclipsing Binary stars. 6

Tony Vale

tony.vale@hotmail.co.uk

This report lists recent timings of minima of various eclipsing binaries. The observations from which the timings were obtained have all been posted to the BAAVSS photometric database.

Timings

Star	HJD of Min	Filter	Error	Type of Minimum
MM Cas	2460006.36126	V	0.00300	Primary
SV Cam	2459992.38641	V	0.00060	Primary
AH Vir	2460003.56499	V	0.00050	Secondary
AL Cam	2459998.40939	V	0.00020	Primary
TY Boo	2460027.51860	V	0.00050	Secondary
TW Cas	2459902.45918	V	0.00120	Primary
TZ Boo	2460038.56276	V	0.00150	Secondary
AW Vir	2460056.39989	V	0.00025	Secondary
RS CVn	2460037.58288	V	0.00125	Primary
TU Boo	2460054.51187	V	0.0008	Secondary
AZ Vir	2460052.55210	V	0.0003	Secondary

The observations from which these timings were obtained were made from November 2022 to April 2023 using a 102mm refractor and an ASI 183MM-Pro cooled mono CMOS camera and a V band filter. The timings were extracted using Bob Nelson's *Minima* software.

Below is the light curve from which the timing of the minimum of RS CVn, included in the above list, was determined. The observations began at about 10pm on 2nd April and ended 7 hours later. This is the third year I have been able to obtain timings for this star and these are shown below, in red, on the O-C Gateway of the Czech Astronomical Society. As you can see, the reduction in the period which has been taking place over the last 60 years or so, is continuing.

Light Curve for RS CVN

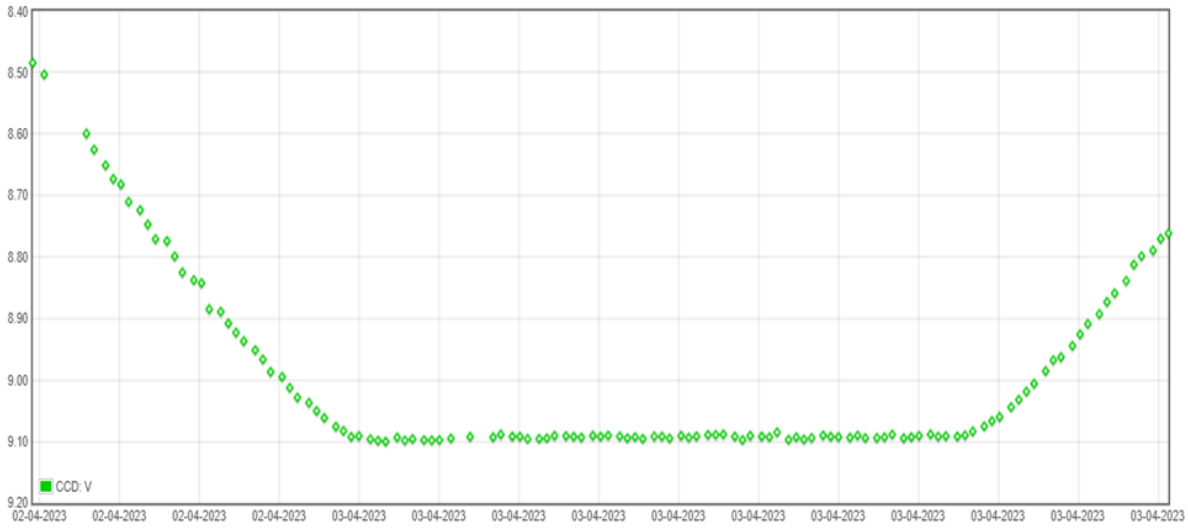

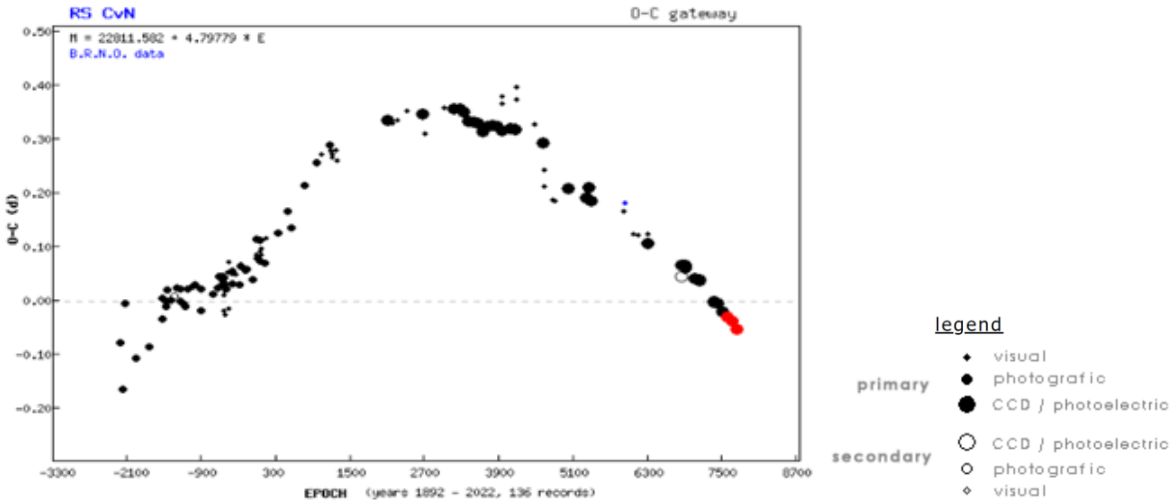

SUMMER MIRAS

M = Max, *m* = min.

W And	M=Aug
RW And	*m*=Jun
R Aqr	M=Aug
R Aql	*m*=Jly
UV Aur	*m*=Aug
X Cam	M=Aug/Sep
	m=Jun
SU Cnc	*m*=Aug
RT CVn	*m*=Aug
S Cas	*m*=Jun/Jly
o Cet	M=Jun
R Com	M=Jly
S CrB	M=Jly
V CrB	M=Aug/Sep
W CrB	*m*=May/Jun
chi Cyg	M=Jun
S Cyg	*m*=Jun
V Cyg	*m*=Aug
SS Her	M=Aug
	m=Jun/Jly
SU Lac	*m*=Jly/Aug
RS Leo	M=Jly
X Lyn	*m*=May/Jun
X Oph	M=Aug
T UMa	*m*=Jun/Jly

Source BAA Handbook

BAA VSS
Section Meeting

Saturday September 2nd, 2023

The Humfrey Rooms
10 Castilian Terrace,
Northampton NN1 1LD.

10:30 - 17:30

Speakers include…

Sean Albrighton, David Conner,
Robert Januszewski,
Dr. Mark Kidger, Dr. Christopher Lloyd,
Robin Leadbeater and Phil Masding,
Mike Poxon, John Toone

No advanced booking required.

Check VSS Web Page for final details.

Section Publications

Hard Copy Charts	Order From	Charge
Telescopic	Chart Secretary	Free
Binocular	Chart Secretary	Free
Eclipsing Binary	Chart Secretary	Free
Observation Report Forms	Director/Red Star Co-ordinator	Free
Chart Catalogue	Director	Free
Binocular VS charts Vol 2	Director or BAA Office	Free

Charts for all stars on the BAAVSS observing programmes are freely available to download from the VSS Website www.britastro.org/vss

Contributing to the VSSC

Written articles on any aspect of variable star research or observing are welcomed for publication in these circulars. The article must be your own work and should not have appeared in any other publication. Acknowledgement for light curves, images and extracts of text must be included in your submission if they are not your own work! References should be applied where necessary. Authors are asked to include a short abstract of their work when submitting to these circulars.

Please make sure of your spelling before submitting to the editor. English (not US English) is used throughout this publication.

Articles can be submitted to the editor as text, RTF or MS Word formats. Light curves, images etc. may be submitted in any of the popular formats. Please make the font size for X & Y axes on light curves large enough to be easily read.

Email addresses will be included in each article unless the author specifically requests otherwise.

Deadlines for contributions are the 15th of the month preceding the month of publication. Contributions received after this date may be held over for future circulars. Circulars will be available for download from the BAA and BAAVSS web pages on the 1st day of March, June, September and December.

Deadline for the next VSSC is August 15th, 2023.

BAA www.britastro.org
BAAVSS www.britastro.org/vss
BAAVSS Database https://www.britastro.org/photdb/
BAA Spectroscopic Database https://britastro.org/specdb/
BAAVSS Circular Archive http://www.britastro.org/vss/VSSC_archive.htm

Section Officers

Director
Prof. Jeremy Shears
Pemberton, School Lane, Tarporley, Cheshire CW6 9NR
Tel: 07795 223869 E-mail bunburyobservatory@hotmail.com

Secretary
Bob C. Dryden
21 Cross Road, Cholsey, Oxon OX10 9PE
Tel: 01491 201620 E-mail visual.variables@britastro.org

Chart Secretary
John Toone
Hillside View, 17 Ashdale Road, Cressage, Shrewsbury SY5 6DT
Tel: 01952 510794 E-mail enootnhoj@btinternet.com

Pulsating Stars Co-ordinator
Shaun Albrighton
4 Walnut Close, Hartshill, Nuneaton, Warwickshire CV10 0XH
Tel: 02476 397183 E-mail shaunalbrighton93@gmail.com

CV's & Eruptive Stars Co-ordinator, Circulars Editor & Webmaster
Gary Poyner
67 Ellerton Road, Kingstanding, Birmingham B44 0QE
Tel: 07876 077855 E-mail garypoyner@gmail.com

Nova/Supernova Secretary
Guy Hurst
16 Westminster Close, Basingstoke, Hants RG22 4PP
Tel: 01256 471074 E-mail guy@tahq.org.uk

Eclipsing Binary Secretary
Des Loughney
113 Kingsknowe Road North, Edinburgh EH14 2DQ
Tel: 0131 477 0817 E-mail desloughney@blueyonder.co.uk

Database Secretary
Andy Wilson

Tel: 01934 830683 E-mail andyjwilson_uk@hotmail.com

Telephone Alert Numbers for Nova and Supernova discoveries telephone Guy Hurst. If answering machine leave a message and then try Denis Buczynski 01862 871187. Variable Star alerts call Gary Poyner or post to BAAVSS-Alert – **but please make sure that the alert hasn't already been reported**.